Journal of Solid State Electrochemistry (2022) 26:1897–1917
https://doi.org/10.1007/s10008-022-05228-5

REVIEW PAPER

Mechanisms of electrochemical nitrogen gas reduction to ammonia under ambient conditions: a focused review

Anjali Kaiprathu[1] · Parthiban Velayudham[1] · Hanan Teller[1] · Alex Schechter[1,2]

Received: 30 May 2022 / Revised: 14 June 2022 / Accepted: 14 June 2022 / Published online: 29 June 2022

Abstract

Electrocatalytic nitrogen reduction reaction (E-NRR) to ammonia is becoming a major topic of interest in the field of large-scale energy storage from renewable sources and water. This approach is considered as an alternative route of ammonia production that could replace the high energy demanding and polluting Haber–Bosch process or high pressure stored hydrogen from electrolysis. This focused review covers different recent aspects of ammonia production via E-NRR electrocatalysis, including the challenges of E-NRR, reaction mechanisms, different materials of E-NRR catalysts such as noble metal-based, non-noble transition metal-based oxides, nitrides, carbides, and hetero-atom-based catalysts, emphasizing bifunctional catalysts reacting at ambient pressures and temperatures, which were not included in previous reviews. In addition, we discuss important issues concerning the commonly used experimental setup, testing protocols, and various NH_3 quantification methods. The various fundamental and applied research methodologies summarized in this review can serve to promote efficient research on electrocatalytic nitrogen reduction and ammonia production, making it a promising future energy storage as a synthetic alternative fuel.

Keywords Energy conversion · Bifunctional catalysts · Nitrogen reduction reaction · Electrocatalyst

Introduction

The ongoing surge in the cost of petroleum-based fuels indicates both an unsustainable demand as well as a depletion in finite crude oil reservoirs [1]. In addition, the widespread infrastructure development and the overwhelming consumption of fossil fuels have resulted in a series of environmental and economic issues such as air pollution, global warming, and geopolitical frictions [2]. Therefore, the need for intensive scientific research and development for exploiting carbon-free, clean energy and fuel is of high priority. These clean energy technologies mostly depend on the electrochemical reactions associated with the abundant species in the earth's atmosphere such as N_2, H_2O, and O_2. Sustainable and environmentally friendly nitrogen and water energy cycles can be established through nitrogen reduction reaction (NRR), ammonia oxidation reaction (AOR), oxygen evolution reaction (OER), and oxygen reduction reaction (ORR) [3]. Among these various methods, electrocatalytic NRR (E-NRR) is an emerging route for ammonia (NH_3) production [4]. Ammonia is one of the major chemical commodities which plays a vital role in the global economy via chemical and hydrogen storage industries [5]. In addition, NH_3 is a promising substitute for hydrogen in fuel cell energy conversion technology since it comprises high hydrogen content (17% compared to 12.5% and 13% in methanol and ethanol, respectively), it is a carbon-free fuel, and it liquefies under low pressures of 8–10 bars at ambient temperatures, thus may be stored as a liquid at about 10 atm at room temperature [6, 7]. Almost 200 million tons of ammonia (NH_3) are produced annually for industrial and agricultural applications, and more than 80% of it is used for the manufacturing of artificial fertilizers and various industries such

To Prof. Doron Aurbach, for years of mentoring generations of scientists in academia, industry, and worldwide. Acknowledgment of your outstanding breakthrough contributions in a wide range of electrochemistry, batteries, and material chemistry studies and for many years of friendship.

✉ Alex Schechter
salex@ariel.ac.il

[1] Department of Chemical Science, Ariel University, 40700 Ariel, Israel

[2] Development Centre for Renewable Energy, New Technology Centre, West Bohemia University, West Bohemia, Pilsen, Czech Republic

as pharmaceuticals, dye industry, and explosives [8, 9]. German scientist Fritz Haber started the research on ammonia production in 1904. Later, in 1918, Haber patented the synthesis of ammonia, and he was awarded the Nobel Prize in Chemistry for this invention [10]. In 1910, Alwin Mittasch successfully synthesized NH_3 using the promoted iron-based catalyst [11]. Afterward, in 1931, Carl Bosch was awarded a Nobel Prize for the scale-up process of ammonia synthesis to the industrial level [10, 12, 13]. Thus, today's process is known as the Haber–Bosch process (HBP) [14]. At present, the only industrial method for NH_3 production is this process, which produces around 200 million tons of NH_3 per year [15]. In this method, a mixture of hydrogen (H_2) and nitrogen (N_2) gases is being passed over an iron-based catalyst. Steam reforming of coal and/or natural gas to produce the inlet H_2 leads to 1.87 tons of the greenhouse gas (CO_2) released per 1 ton of NH_3. The exothermic N_2 reduction reaction requires temperatures of 300–500 °C to improve the kinetics and a pressure of 150–200 atm [16–18]. Thus, this method is highly energy demanding and not environmentally friendly due to the emission of CO_2 [19, 20]. Therefore, there is an urgent need for an alternative, green, and sustainable method for the production of efficient and clean energy. Recent years have witnessed the selective attraction among researchers in the direction of sustainable ammonia production via nitrogen reduction reactions (NRRs) [3, 21], as an alternative method to the conventional HB process. One of the most promising methods is the electrocatalytic nitrogen reduction process using noble metal-based, non-noble transition metal-based oxides, nitrides, carbides, hetero-atom-based electrocatalysts, and bifunctional catalysts which utilize a synergistic effect between two components to enhance the E-NRR and increase its efficiency. The key topics in this review include various catalyst systems including bifunctional electrocatalysts, reported for NRR with the supporting mechanisms, challenges of NRR, and finally the commonly used experimental setup, testing protocols, and various NH_3 quantification methods. We believe that the various approaches summarized in this review may provide valuable insights to promote efficient research on electrocatalytic nitrogen reduction.

Fundamental understanding of electrochemical ammonia synthesis

Basic challenges of E-NRR

Various methods such as electrochemical nitrogen reduction reaction (E-NRR) [22–25], electroreduction of nitrate [26, 27], photocatalytic NRR [28], plasma chemical NRR [29], biochemical and photocatalytic NRR [30] have been proposed for the alternative synthesis of ammonia. The photocatalytic and electrocatalytic N_2 reduction using water as the hydrogen source is regarded as renewable approaches under ambient conditions, offering a promising way for green and sustainable NH_3 production [17, 31, 32]. The ideal scenario for these processes requires a catalyst to ensure a high rate and selectivity, which remains a coveted goal. In the past decades, catalysis by electrochemical methods was the heart of several energy production and storage systems, which gained great attention and opened a new window for NH_3 synthesis [33]. The chemisorption of a reactant on active sites and the subsequent activation process induced by the electron transfer demonstrate an alternative conversion route in which the free energy barrier is low [15, 34]. Therefore, significant efforts have been devoted recently to developing a novel catalyst design that evades the large energy barrier of N_2 reduction. However, its widespread employment is still hindered by various factors, such as low yields of NH_3, costly electrolytes, and harsh operating conditions [35, 36]. The inertness of nitrogen (N_2) is due to the strong triple bonding between two N atoms (N≡N) with a bonding energy of 940.95 kJ mol^{-1} and high ionization energy of 15.6 eV [37, 38], non-polarity, and negative electron affinity (− 1.9 eV). These properties result in large overpotential and a very low Faradaic efficiency (FE) (typically < 10%) for NRR [18, 39]. In addition, the first protonation of N_2 which is an endothermic process with $\Delta H^0 = +37.6$ kJ mol^{-1} is thermodynamically hindered [15, 37, 40–42]. It is worth noting that although the first protonation of N_2 on many catalyst systems is endothermic, subsequent protonation to form NH_3 is relatively easy. Thus, the overall Gibbs free energy change of the NRR is negative [43], as exemplified by the conversion of N_2 to NH_3 by natural nitrogenase systems, the Haber–Bosch process, photocatalysis, and electrocatalysis. In addition, the large energy gap, about 10.82 eV, between the highest occupied and the lowest unoccupied molecular orbitals of N_2 does not favor the one- or two-electron transfer process and therefore endows the NRR with sluggish kinetics where most protons and electrons have preferred tendency towards a competing cathodic H_2 generation [44, 45]. Subsequently, selectivity remains a major challenge for the multi-electron and multi-proton NRR pathways in competing with the dominant HER for active catalysts. Theoretically, the transition metal-based catalysts overcome the kinetic limitation of N≡N activation through their π-back-donation process. Transition metals have the unoccupied d-orbitals which can receive the N_2 lone-pair electrons, and at the same time, the occupied d-orbitals of transition metal atoms can donate their electrons to the antibonding orbital of N_2. This electron transfer weakens the N≡N bond [46]. But practically, the transition metals can also facilitate the formation of a metal−H bond, leading to undesirable side reactions [47]. In summary, the NRR competes aggressively with the hydrogen evolution reaction (HER) which lowers the FE. As

a result, the majority of the transition metal-based catalysts can give 10^{-8} mol cm^{-2} s^{-1} or below NH_3 producing rates and Faradaic efficiencies (FEs) lower than 10%, which is far from the necessary amount needed for practical application in the industry [26, 48]. Giddey et al. suggested that for commercial and industrial applications, we need to have an NH_3 formation rate near 10^{-6} mol cm^{-2} s^{-1} and FE of more than 50% [49].

The E-NRR involves multistep N_2 protonation and multielectron transfer, as illustrated below [24, 38, 50, 51];

$$N_2 + H^+ + e^- \leftrightarrow N_2H \qquad E^0 = -3.20 \text{ V vs RHE} \quad (1)$$

$$N_2 + 2H^+ + 2e^- \leftrightarrow N_2H_{2(g)} \qquad E^0 = -1.10 \text{ V vs RHE} \quad (2)$$

$$N_2 + 4H^+ + 4e^- \leftrightarrow N_2H_{4(g)} \qquad E^0 = -0.36 \text{ V vs RHE} \quad (3)$$

$$N_2 + 6H^+ + 6e^- \leftrightarrow 2NH_{3(g)} \qquad E^0 = -0.148 \text{ V vs. RHE} \quad (4)$$

$$N_2 + 6H_2O + 6e^- \leftrightarrow 2NH_{3(g)} + 6OH^- \qquad E^0 = 0.09 \text{ V vs. RHE, pH} = 14 \quad (5)$$

$$N_2 + 4H_2O + 4e^- \leftrightarrow N_2H_{4(g)} + 4OH^- \qquad E^0 = -0.334 \text{ V vs. RHE, pH} = 14 \quad (6)$$

$$N_2 + e^- \leftrightarrow N2^-_{(aq)} \qquad E^0 = -3.37 \text{ V vs. RHE, pH} = 14 \quad (7)$$

$$2H + +2e^- \leftrightarrow H_{2(g)} \qquad E^0 = 0 \text{ V vs. RHE, pH} = 0 \quad (8)$$

$$2H_2O_{(l)} + 2e^- \leftrightarrow H_{2(g)} + 2OH^- \qquad E^0 = 0 \text{ V vs. RHE, pH} = 14 \quad (9)$$

Equations (1)–(3) show that the main hindrance to the electrochemical conversion of N_2 to NH_3 is the first one-electron reduction/protonation of N_2, which is the rate-determining step. The subsequent six and four-electron reductions are comparatively easier. When comparing Eqs. (7) and (1), it is clear that the activation of N_2 via H binding is more favorable than that via reduction to N_2^- as the latter requires more severe conditions (pH = 14) and occurs at higher potential. The two groups of reactions described by Eqs. (4)/(8) and (5)/(9) show that in addition to the E-NRR steps, the competitive HER is unavoidable in aqueous solutions and it is the main side reaction, charge consuming of E-NRR systems. In addition, if N_2H_4 cannot be further protonated on the catalyst surface to break the remaining N–N bond, the formation of this specie may compete with the generation of NH_3 (Eqs. (3) and (6)). The relatively large equilibrium potential, numerous intermediate states, and widespread side reactions (mainly the HER) of the E-NRR greatly hinder the mechanistic investigation. Hence, higher requirements are put forward for an improved design of E-NRR catalysts and the overall optimization of the electrochemical system efficiency.

Mechanisms of E-NRR

E-NRR is one of the typical heterogeneous reactions, which involves three basic steps: adsorption of dinitrogen molecule at the catalytically active site on the surface of the catalyst, then hydrogenation, and finally the desorption of NH_3 molecules (or other intermediates). The E-NRR mechanisms are generally divided into associative and dissociative mechanisms based on the different hydrogenation processes such as protonation and reduction sequences and the breaking of the N≡N bond as shown in Fig. 1 [51, 52]. In the associative mechanism, N_2 molecule is adsorbed on the catalyst surface, and then, the hydrogenation process proceeds. Here, the hydrogenation process consists of various approaches such as distal(end-on), alternating, and enzymatic pathways [53]. In the distal pathway, the hydrogenation preferentially takes place on the N atom far away from the surface of the catalyst. When the first NH_3 molecule is formed and released, the N atom bound to the surface of the catalyst gets hydrogenated subsequently and produces the second NH_3 molecule. In the alternating pathway, the hydrogenation happens on two nitrogen atoms alternatively, and the N≡N bond breaks at the last step with the formation of the first NH_3 molecule, which leaves one NH_3 molecule behind [54, 55]. In the enzymatic pathway, which is different from the alternating one, the N_2 adsorbs sideways on the surface of the catalyst in the first step. The following hydrogenation steps are similar to those in the alternating pathway [56]. In the dissociative mechanism, the N≡N bond is broken in the process of adsorption, leading to the adsorption of individual N atoms separated by a distinct distance. The hydrogenations on each N atom in the following steps result in the formation of ammonia, which is released at the last step. Moreover, the dissociate pathway is applied in industrial

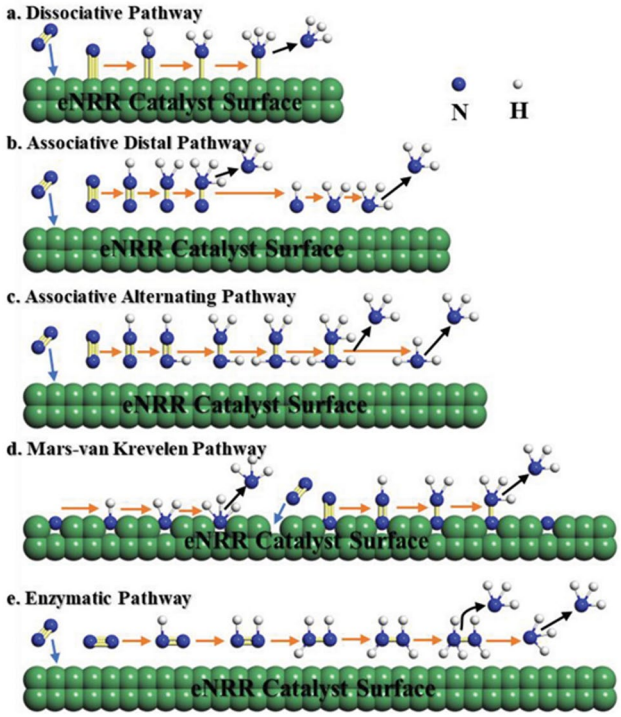

Fig. 1 Schematic diagram of dissociative and associative pathway, Mars-van Krevelen mechanism, and surface hydrogenation mechanism. Reproduced with permission [52]

production processes, mainly in the Haber–Bosch process, featuring the cleavage of the N≡N bond of N_2 on the catalyst surface at high temperature to form activated atomic nitrogen (N*) that is subsequently hydrogenated to generate NH_3. The conversion of N_2 to NH_3 via this pathway is driven by high thermodynamic energy and is therefore difficult to implement under ambient conditions. Recently, a new mechanism that is completely different from the dissociative and associative pathways has been proposed for the conversion of N_2 to NH_3, i.e., Mars-van Krevelen mechanism (the MvK pathway) [57]. In general, the formation of NH_3 on the surface of transition metal nitrides is believed to follow the MvK pathway. According to this mechanism, the N atom on the transition metal nitride is reduced to NH_3. The N_2 provided by the environment fills the vacancy of the extracted lattice N atoms to complete catalyst recovery and prepare for a new reaction [58]. The MvK mechanism has been recognized by researchers and compared with the associative pathway to reveal that in the former case, N_2 is electrochemically converted into NH_3 with a lower overpotential [59]. Given the poor solubility of N_2 in water, the MvK mechanism can compensate for the lack of N_2 supply to a certain extent. This compensation can be attributed to the large area effect of the catalyst that can capture traces of N_2 in the electrolyte to fill the N defects.

Research on the mechanism of N_2 conversion to NH_3 in the E-NRR remains largely theoretical, with only a limited number of reports containing fundamental experimental data. At present, some detection methods can be introduced into the E-NRR to determine the key steps of the N_2 to NH_3 conversion. For instance, in situ electrochemical infrared and in situ electrochemical Raman spectroscopy can be used to track subtle real-time changes in the electrolyte and catalysts on the working electrode. Moreover, experimental data analysis can be combined with theoretical calculations to elucidate the type of NH_3 formation mechanism occurring on a specific catalyst, which will have a far-reaching influence on E-NRR development. Despite the significant experimental and theoretical studies on the E-NRR, the selectivity for proton-coupled electron transfer (PCET) and sequential proton-electron transfer (SPET) pathways in the conversion of N_2 to NH_3 remains unclear. It is often assumed that the PCET pathway occurs on the surface of solid metal catalysts, whereas certain works also show the importance of the SPET pathway under these conditions [38, 60, 61]. Kumar et al. used theoretical calculations to show that the ammonization of N_2 in the E-NRR preferentially follows the SPET pathway; specifically, H^+ ions attack the activated N_2, and electrons are then introduced into the obtained positively charged intermediate [62]. The potential barrier of proton transfer in the SPET pathway (28.78 kcal mol^{-1}) is lower than that in the PCET pathway (31.03 kcal mol^{-1}). Although the former pathway is preferred in the E-NRR, the selectivity for these two pathways depends on the pH of the environment [60]. To avoid the undesired occurrence of the HER, the above studies did not consider pH. Therefore, regarding the selectivity of PCET and SPET pathways, more detailed theoretical calculations are needed to optimize the physical and chemical properties of E-NRR catalysts. Therefore, further research is needed for more sustainable and cost-effective methodologies to produce NH_3 to support the growing world demand.

Recent progress in the theoretical study of electrocatalysts for E-NRR

Transition metal catalysts

Favorable chemisorption of N_2 and its subsequent activation through hydrogenation on the active catalytic center are the primary criteria for designing efficient electrocatalysts for E-NRR. Improving the selectivity of NRR by limiting the competitive HER on the catalyst center and durability of the catalysts are also key factors to be considered while designing electrocatalysts for E-NRR applications. Recent advancement in the computational and modeling field is very helpful in designing such electrocatalyst and exploring the

reaction mechanisms by determining the reaction-free energies. Norskov et al. theoretically studied the free energies for the adsorption and reduction of N and H atoms on stepped and flat surfaces of various transition metal surfaces using DFT calculations to scrutinize the suitable metal surface for electrochemical ammonia synthesis under ambient conditions [41]. They have predicted that the surfaces of metals such as Mo, Fe, Rh, and Ru, located at the top of the volcano plot, are predicted to be more active in E-NRR. But these materials are also predicted to be more active in promoting the competitive HER, thus leading to a poor FE of ammonia production. On the other hand, the flat surface of early transition metals such as Sc, Y, Ti, and Zr are expected to show higher ammonia production as these elements strongly bond with N-adatoms than the H-adatoms at the expense of increasing the applied bias from − 1 to 1.5 V. In contrast, the elements located on the right side of the volcano diagram, such as Rh, Ru, Ir, Co, Pt, and Ni, strongly adsorb H-adatoms and thus tend to show more selectivity towards HER than NRR. Xu et al. used the Vienna Ab Initio Simulation Package (VASP) software based on DFT to explore the d-block metal atoms embedded in arsenene for different transition systems of phosphorus coordination as potential E-NRR catalysts [63]. They have found that the Nb@P_3-Ars system is thermodynamically stable, with a low E-NRR overpotential which facilitates the efficient reduction of N_2. Qian et al. studied Fe-$Ti_3C_2O_2$ catalysts using DFT calculations [64]. They have found that the charge transfer from Fe to N_2 molecules weakens the N–N bond making it a potential E-NRR catalyst. Doping with F or S atoms reduces the limiting potential of the two potential-limiting steps in the reduction reaction. Guo and Jiao studied different diatomic catalysts by density functional theory calculations and concluded that FeTi@Pc (Pc = phthalocyanine) catalyst has the best catalytic activity with the limiting potential of − 0.37 V and selectivity for NRR reaction [65].

Transition metal oxide catalysts

Transition metal oxide (TMO)-based catalysts have been studied for various electrochemical reactions, including the E-NRR owing to their variable oxidation states, ease of synthesis, chemical stability, and low cost. In search of efficient TMOs to boost the E-NRR activity under ambient conditions, Höskuldsson et al. performed the DFT calculations on the (110) facets of NbO_2, RuO_2, RhO_2, TaO_2, ReO_2, TiO_2, OsO_2, MnO_2, CrO_2, IrO_2, and PtO_2 in the rutile structure and proposed a volcano-type plot of the applied potential versus the binding energy of NNH intermediates (Fig. 2) [66]. The oxides located at the left leg of the volcano map preferably adsorb N_2 and NNH, while the oxides located at the right leg strongly bond H-adatoms. Their study predicted that higher yields of ammonia formation are possible by employing the ReO_2 and TaO_2 as these TMO surfaces favor NNH adsorption over hydrogen adsorption. Further, IrO_2 was found to be the most active catalyst for E-NRR with the lowest onset potential of − 0.36 V, but adsorbed hydrogen atoms might poison its surface.

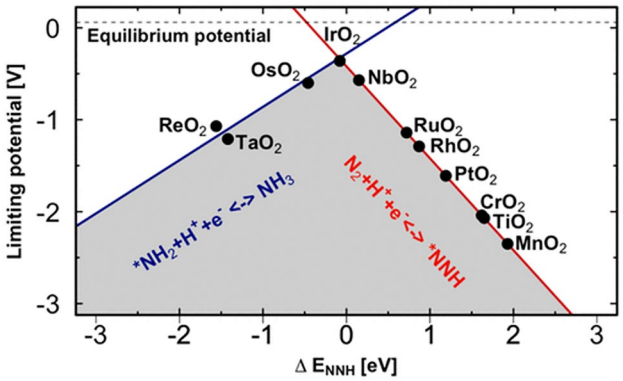

Fig. 2 Potential determining step for electrochemical ammonia formation on each metal oxide is plotted against the binding energy of NNH. The lines are constructed using scaling relations. Reproduced with permission [66]

Miscellaneous catalysts and supports

Several theoretical studies also predicted the activity of various transition metal nitrides [67], iron boride [68], single and double transition metal atom catalyst supported on graphyne [69], graphdiyne [70], MoS_2 [71], MXene [72], and g-CN [73], for electrochemical ammonia synthesis under ambient conditions. For instance, Zhai et al. systematically investigated a series of single transition metal atoms supported on MoS_2 nanosheets (TM@MoS2) for their E-NRR performance [71]. DFT calculations study revealed that the Re supported on MoS_2 (Re@MoS_2) can be a potential NRR catalyst at potentials lower than − 0.43 V with high NRR selectivity over the competing HER. In another study, Lv et al. examined the potential of various transition metal double atom catalysts (TM-DACs) supported on the graphitic carbon nitride (g-CN) by DFT calculations for E-NRR applications [73]. Their study predicted that the Fe–Fe distributed on g-CN (Fe_2/g-CN) can achieve the highest theoretical Faradaic efficiency of 100% with the lowest applied potential of − 0.13 V. The synergistic effect of dimer Fe sites and g-CN thus promoting the chemisorption of N_2 and its successive activation through hydrogenation with good selectivity and stability is mainly responsible for the highest activity of Fe_2/g-CN among the 23 transition metal centers studied. The enhancement of the electroactivity of different E-NRR

catalyst types utilizing defect engineering, by changing the electronic states as well as creating additional active sites for the reduction reactions, was recently reviewed by Zhang et al. [74]. Zhao et al. investigated the potential application of metal-free single B atom-doped C_5N_2 electrocatalyst for NRR employing the DFT calculations. Their study evidenced that B is doped to the interstitial site of C_5N_2 and the resultant catalyst activates the N_2 via acceptance-donation process. Further, N_2 is getting reduced with low overpotential of 0.38 V via alternating mechanism [75]. These important theoretical studies may pave the way to design novel and efficient electrocatalysts that deliver higher ammonia production rates with high selectivity.

Summary of various electrocatalysts for E-NRR

Recently, significant efforts have been devoted to designing and fabricating NRR electrocatalysts. The slow reaction kinetics, low Faradaic efficiencies, low production rate, and selectivity toward NH_3 under mild reaction conditions limit the development of commercial applications for NRR electrocatalysts. Therefore, the current research in E-NRR is highly demanding for developing novel efficient electrocatalysts to overcome the challenges. This section will elaborate on the NRR performance of relevant reported electrocatalysts.

Noble metal-based catalysts

Noble metals have excellent electrical conductivity, abundant active polycrystalline surface facets, and unfilled d-electron orbitals for the strong adsorption and binding of N_2 and with a wide range of reactants. Thus, they can be a better candidate for efficient electrocatalysts in many reactions. These electrocatalysts exhibit excellent catalytic properties and are widely used in electrochemical reactions such as hydrogen evolution reaction (HER) and oxygen reduction reaction (ORR) [76]. Thus, it is expected that the Noble metal-based catalysts will exhibit efficient catalytic activity for nitrogen reduction reaction, and there have been many reports of NRR by noble metals such as Pt [77], Ru [78, 79], Rh [80], Au [81, 82], and Pd [83].

Gold (Au) is considered one of the precious stable metals which have been extensively used as a potential catalyst for several reactions. Nowadays, gold-based catalysts are extensively studied for E-NRR. This is because the unoccupied d-orbital of Au can accept the lone pairs of electrons from N_2 without much energy. In addition, the HER activity of Au-based materials is much lower than that of Ru-, Pt-, and Pd-based ones. So, Au-based materials favor the E-NRR over the HER.

Yan and co-workers explored these catalysts for NRR [81]. They synthesized novel tetra-hexahedral gold nanorods (THH Au NRs) with the help of a binary surfactant mixture by seed growth method. The synthesized gold nanorods were enclosed by the stepped (730) facet, composed of (210) and (310) subfacets. Further, they explored its catalytic activity towards E-NRR, which exhibited comparable NRR activity with an NH_3 formation rate of 1.648 μg h^{-1} cm^{-2} at − 0.2 V vs. RHE in 0.1M KOH. Along with NH_3, N_2H_4 is also formed during the reaction with a production rate of 0.102 μg h^{-1} cm^{-2}. Yet, the NH_3 yield, selectivity, and Faradaic efficiency (FE) were too low to meet the requirements of practical applications. The reason for the low NH_3 formation rate may be due to the structure which is detrimental to mass transport, and the possible residual surfactant used in the synthetic process which covers the active sites of the tetra-hexahedral gold nanorods covering the active sites of catalyst, resulting in relatively low NH_3 production rate. The removal of those surfactant molecules and construction of two or three dimension nanostructures might increase the number of free active sites and the efficiency of these catalysts. Nazemi et al. invented hollow gold nanocages (AuHNCs) from silver solid nanocube (AgNC) template without using any surfactant [84]. These gold nanocages have shown the highest NH_3 yield rate of 3.9 μg h^{-1} cm^{-2} at − 0.5 V vs. RHE, with the highest FE of 30.2% at − 0.4 V vs. RHE. In addition, they compared the NRR activity of solid Au nanoparticles with different shapes such as rods, spheres, and cubes and observed that the excellent catalytic activity is shown by cube structure having an increased surface area and the confinement of reactants in the cavity (cage effect). Recently, Wang and co-workers developed a catalyst of uniformly deposited Au on Ni foam (pAu/NF), by a micelle-assisted electrodeposition method, with a porous Au film structure. These catalysts exhibit excellent NRR performance with a greater NH_3 production rate of 9.42 μg h^{-1} cm^{-2} and a FE as high as 13.36% at − 0.2 vs. RHE in 0.1 M Na_2SO_4 under ambient conditions without the formation of any side products [85]. The higher rate of NH_3 formation might be ascribed to the interconnected porous architectonics and rich Au active sites on the Au film with a thickness of 400 nm.

In addition to Au, ruthenium (Ru) also shows high catalytic activity towards NRR attributed to the strong adsorption of *HNNH (the desorption of *HNNH to liberate HNNH from the catalyst surface is energetically uphill by 1.53 eV), or to the easiness to form $*NH_2NH_2$ because of the availability of other lower-energy pathways [86]. An excellent NRR catalytic activity of Ruthenium nanoparticles (Ru NPs) prepared by MacFarlane and co-workers was investigated in 0.1 M HCl. The catalyst exhibited high NH_3 yield rates of 5.5 mg h^{-1} m^{-2} at 20 °C and 21.4 mg h^{-1} m^{-2} at 60 °C at − 0.1 V vs. RHE, while the highest Faradaic efficiency

of ~ 5.4% was realized at $E = +10$ mV vs. RHE. The ability of Ru NPs to catalyze the E-NRR at potentials near or above RHE rendered the H_2 formation as a by-product and improved the NRR selectivity. DFT calculations suggest that the efficient NRR process occurs predominantly on the Ru (001) surfaces via a dissociative mechanism [87]. The Ru single atoms distributed on nitrogen-doped carbon (Ru SAs/N-C) via pyrolyzing the Ru-containing derivative of zeolitic imidazolate frameworks developed by Zeng and co-workers demonstrated highly catalytic activity with NH_3 yield rate of 120.9 μg h^{-1} mg^{-1} and high Faradaic efficiency of 29.6% at − 0.2 V vs. RHE for NRR [88]. This finding became a guide for the study of the uniform distribution of single atomic catalysts to improve the applicability of E-NRR.

Pd-based catalysts were also studied and reported for NRR. Palladium nanoparticles in phosphate buffer solution under ambient conditions exhibited high activity and selectivity with an NH_3 yield rate of ~ 4.5 μg mg^{-1} Pd h^{-1} and a Faradaic efficiency of 8.2% at 0.1 V vs. RHE. DFT calculations suggest that the unique activity of palladium originates from its mitigated hydrogen evolution activity and the Grotthuss-like hydride transfer mechanism on α-palladium hydride that lowers the free energy barrier of N_2 hydrogenation to $*N_2H$, the rate-limiting step for NH_3 electrosynthesis activity [89]. Metalic palladium (Pd) is not suitable to serve as a catalyst for the nitrogen reduction reaction due to its stronger affinity with H atoms than N atoms, which will hinder the adsorption of N_2 on the surface of Pd and promote HER [90]. Noble metal catalysts cannot be used as a benchmark for distinguishing the activity of NRR catalysts, due to the complexity of the nitrogen reaction process and the competition of side reactions. Even though they still exhibit excellent reactivity and selectivity compared to non-noble metal catalysts.

Non-noble metal-based catalysts

Though the noble metal-based electrocatalysts have made a great advancement in their catalytic activity, selectivity, and Faradic efficiency, their wide practical application is still limited due to their high cost, limited availability, and relatively low selectivity towards N_2 [91]. In that direction, the non-noble metal-based electrocatalysts have been extensively used as a potential alternative for noble metal-based electrocatalysts. The low cost, earth-abundant, and unique d-orbital electrons for the π-back donation process of non-noble metal-based catalysts, especially transition metal-based materials lighten a new direction to explore it widely for NRR [92, 93]. The naturally occurring nitrogenase enzymes contain non-noble metal catalytic active sites of Fe and Mo, which play a vital role in biological N_2 fixation to convert nitrogen to ammonia under normal conditions [17, 56, 94, 95]. Therefore, the development of non-noble metal catalysts, inspired by this process, attracted great attention. Sun and co-workers developed MoS_2 nanosheet arrays grown on carbon cloth (MoS_2/CC) and first used it for the NRR under ambient conditions. The catalytic activities in both neutral and acidic conditions were explored resulting in an NH_3 yield rate of 8.08×10^{-11} mol s^{-1} cm^{-1} and 8.48×10^{-11} mol s^{-1} cm^{-2} in neutral and acidic conditions, respectively [96]. Wang and co-workers reported (110)-oriented Mo nanofilm for electrochemical reduction of N_2 at an overpotential of 0.14 V with Faradaic efficiency (FE) of 0.72% [97]. In addition, the rate of NH_3 formation as high as 3.09×10^{-11} mol^{-1} cm^{-2} can be obtained under an applied potential of − 0.49 V vs. RHE. Similarly, the Fe-based catalysts were also well explored for NRR. Zhou et al. reported that the nanostructured iron catalyst in ionic liquids could catalyze NRR under ambient conditions with a high FE of up to 60% and an NH_3 yield rate of 14 mg m^{-2} h^{-1} [98].

Transition metal oxides

Transition metal catalysts such as NbO_2, RuO_2, RhO_2, TaO_2, ReO_2, TiO_2, OsO_2, MnO_2, CrO_2, IrO_2, and PtO_2 also showed appreciable E-NRR activity with selectivity and stability. Theoretical investigation and calculations done by Höskuldsson et al. showed that the (110) facets of ReO_2, NbO_2, and TaO_2 are promising candidates for E-NRR with onset potentials of − 0.57 V, − 1.07 V, and − 1.21 V vs. SHE [66]. Recently, it has been experimentally proved that NbO_2 nanoparticles show excellent E-NRR activity at ambient reaction conditions.. This catalyst exhibited a high rate of NH_3 formation of about 11.6 μg h^{-1} mg^{-1} cat. at − 0.65 vs. RHE with outstanding Faradaic efficiency (FE) of 32% at − 0.60 V vs. RHE [99]. In addition, Nb_2O_5, with a NbO_2 analogous crystal structure, is also an effective electrocatalyst for E-NRR under ambient conditions. It has been demonstrated that the Nb_2O_5 nanofibers achieve a high NH_3 production rate of 43.6 μg h^{-1} mg^{-1} cat. and a high FE of 9.26% at − 0.55 V vs. RHE in 0.1 M HCl [100]. In addition, Kong et al. reported the γ-Fe_2O_3 for NRR in basic aqueous conditions with FE of 1.9% and an NH_3 formation rate of 0.212 μg h^{-1} mg^{-1} at 0 V vs. RHE [101].

Transition metal nitrides

Similarly, transition metal nitrides also show catalytic activity towards E-NRR. The MvK mechanism and DFT calculations were used to screen these catalysts for NRR. The stability of the lattice planes, the N vacancy on the catalyst surface, the catalytic activity, the stability of the nitrides at the onset potential, and the poisoning of the surface vacancy suggest that the most promising nitride catalysts are the (100) planes of rock salt VN and ZrN which

should form ammonia at − 0.51 V and − 0.76 V vs. SHE, respectively [102]. Rong et al. synthesized VN nanosheet array on Ti mesh and explored its NRR activity in 0.1 M HCl at room temperature and atmospheric pressure [103]. The results indicate that VN catalyzes NRR via an MvK mechanism with high electrochemical stability and selectivity. The catalyst achieves a Faradaic efficiency of 2.25% and an NH_3 formation rate of 0.84 μmol s^{-1} m^{-2} at − 0.50 V. The DFT calculations on molybdenum nitride (MoN_2) nanosheets show that the catalyst has some activity for NRR at room temperature [104]. Despite the advantages, nitride-based electrocatalysts may not be a viable choice for E-NRR application in terms of long-term stability. In our previous study, we demonstrated the instability of vanadium-nitride powder in terms of the V and N leaching out to the electrolyte solution, which was evidenced by the chemical and electrochemical analysis in acidic, neutral, and alkaline aqueous electrolytes [105]. In acidic and neutral electrolytes, the nitrogen was chemically leached out at rates of 4.24×10^{-9} mol h^{-1} mg^{-1} and 3.77×10^{-9} mol h^{-1} mg^{-1}, respectively, while nitrogen was leached out electrochemically at higher rates of 3.85×10^{-8} mol h^{-1} mg^{-1} in HCl and 4.72×10^{-8} mol h^{-1} mg^{-1} in Na_2SO_4. Similarly, rates of 1.28×10^{-9} mol h^{-1} mg^{-1} and 3.86×10^{-10} mol h^{-1} mg^{-1} were observed for the chemical leaching out of vanadium, while its electrochemical leaching rates were 2.62×10^{-8} mol h^{-1} mg^{-1} and 5.70×10^{-8} mol h^{-1} mg^{-1} in HCl and Na_2SO_4, respectively. Therefore, careful initial testing with rigorous control experiments is highly desirable while employing the transition metal nitrides and other types of nitrogen-containing catalysts for E-NRR application, to avoid overestimation of their activity and to realize long-term stability.

Carbon-based catalysts

The carbon-based catalysts have a unique position in electrocatalysis, irrespective of whether they are directly involved in the catalytic process or used as carriers for hybrid materials. The porous and layered structure of carbon materials, their excellent electrical conductivity, abundant possibilities for surface engineering such as defect introduction and heteroatom doping, and low cost made these materials irreplaceable catalysts for electrocatalysis [106]. The carbon-based E-NRR catalysts are mainly divided into pure carbon, single heteroatom-doped carbon, and multiple heteroatom-doped carbon materials [107]. The surface defects present in the carbon-based materials often become the active sites for the N_2 adsorption. In addition, the doping of heteroatom such as N, B, and P often leads to changes in the carbon material band gap, charge density, and spin density, thereby achieving the synergistic catalytic activity of the E-NRR [42]. Li et al. have shown that the catalytic activity of defect-rich CC-450 by simple heat treatment of commercial carbon cloth (CC), for NRR, is less than that of the defect-free CC [108]. Many studies on carbon-based materials for E-NRR suggest that doping with heteroatoms having a strong electron affinity such as N, B, and oxygen group elements can increase the positive charge density of adjacent C atoms and thus stimulate the E-NRR activity of carbon-based materials [109]. To comprehensively present the real status of E-NRR catalyst research, Table 1 lists the active catalysts for E-NRR reported in recent reports and have not been discussed in detail herein.

Electrocatalysts with bifunctional active sites

Factors such as sluggish kinetics due to the multiple proton-electron transfer steps, competing HER, strong N–N triple bond of N_2, and N_2 poor solubility in aqueous electrolytes severely affect the ambient condition electrochemical ammonia synthesis and lead to the poor FE. Designing an electrocatalyst that plays a bifunctional role can be considered as an effective strategy to tackle these limitations associated with E-NRR as exemplified in Fig. 3 with the Pt–Ru catalyst system. Secondary active sites or components of such bifunctional catalysts are expected to play a crucial role in boosting the N_2 activation via facile hydrogenation and impede the HER, thus can help in achieving higher ammonia production with excellent NRR electrochemical selectivity.

For instance, Lv et al. fabricated PdO/Pd heterojunction supported on carbon nanotubes (PdO/Pd/CNTs) by ultraviolet laser irradiation of PdO/CNTs in distilled water [110]. Although both the Pd and PdO can absorb subsurface H to imitate α-PdH, the PdO exhibits superior affinity to H through the surface oxygen atoms (− 3.22 eV) than Pd (− 2.89 eV). Hence, the Pd in PdO/Pd/CNT heterojunction constructed in this study can strongly adsorb N_2 and form the chemisorbed Pd–N bond while PdO absorbs the activated H protons to imitate α-PdH, which is a stable phase for N_2 hydrogenation under operating potentials. The synergistic effect arising from the PdO and Pd bifunctional active sites greatly decreases the transfer distance between the activated N_2 and H protons, thus leading to the kinetically favorable NRR process on PdO/Pd/CNT heterojunction composites. As the PdO-Pd interface plays a crucial role in NRR performance, the effect of different amounts of PdO-Pd interfaces in PdO/Pd/CNTs was also optimized by controlling the irradiation time. As a result, the PdO/Pd/CNTs irradiated for 10 min with an optimal ratio of Pd (18%) to PdO (82%) exhibited the highest NH_3 yield of 18.2 μg $mg^{-1}_{catal.}$ h^{-1} with FE of 11.5% at 0.1 V vs. RHE.

The bifunctional activity of the Fe_2O_3-TiO_2 electrocatalyst for facile electrochemical ammonia synthesis directly from nitrogen and air in an alkaline electrolyte under ambient conditions was demonstrated by Manjunatha et al.

Table 1 Summary of NRR activity of various catalysts reported very recently

Catalyst	Electrolyte	Potential (vs RHE) (V) (at maximum rate of NH_3 formation)	Rate of NH_3 Formation ($\mu g\ h^{-1}\ cm^{-2)}/\mu g\ h^{-1}\ mg_{cat}$)	Potential (vs RHE) (V) (at maximum FE)	FE (%)	Ref.
RuPt/C	1 M KOH	0.023	38.8/-	0.123	13.2	[113]
PdCu/NC	0.05 M H_2SO_4	− 0.45	-/69.2	− 0.45	24.8	[146]
FeNi@CNS nanocomposite	0.1M Na_2SO_4	− 0.2	16.52/-	− 0.2	9.83	[147]
$MoS_{2-x}O_y$) nanosheets	0.1M HCl	− 0.35	35.0/-	− 0.3	9.86	[148]
Ti_2N nitride MXene	0.1M HCl	− 0.25	11.33/-	− 0.35	19.85	[149]
Li-intercalated TiO_2 nanosheets	0.5 M $LiClO_4$	− 0.4	-/8.7	− 0.4	18.2	[150]
Fe_2O_3-TiO_2	1 M KOH	− 0.177	1.07/-	23	1.9	[111]
Boron carbonitride (BCN)	0.05 M Na_2SO_4	− 0.6	8.39/-	− 0.3	9.87	[151]
Reduced graphene oxide (DrGO)	0.1M HCl	− 0.116	-/7.3	− 0.166	10.8	[152]
Vulcanized FeMoO	0.1M Na_2SO_4	− 0.39	-/31.93	− 0.39	30.9	[153]
Fe ion grafted on MoO_3 nanorods	0.1M Na_2SO_4	− 0.6	-/9.66	− 0.6	13.9	[154]
Ag-doped Cu nanosheets	0.1M Na_2SO_4	− 0.4	-/61.5	− 0.4	20.9	[155]
Cobalt single atom catalyst	0.01 M HCl	− 0.1	-/67.6	− 0.1	56.9	[156]
Ag_4Ni_2 nanoclusters	0.1M HCl	− 0.2	-/23.32	− 0.2	78.97	[157]
Single Mo atoms anchored on nitrogen-doped graphene	0.05 M H_2SO_4	− 0.05	-/3.6	− 0.05	50.2	[158]

(Fig. 4) [111]. At an applied potential of 0.023 V vs. RHE, the NH_3 yield of 1.25×10^{-8} mmol $mg^{-1}\ s^{-1}$ was realized with Fe_2O_3/TiO_2/C electrocatalyst, at an overpotential of just 34 mV. This rate increased to 2.7×10^{-7} mmol $mg^{-1}\ s^{-1}$ at − 0.577 V vs. RHE. The authors confirmed that Fe_2O_3/TiO_2/C exhibits a superior nitrogen reduction reaction activity compared to Fe_2O_3 alone and support the bifunctionality of Fe_2O_3 together with TiO_2 (see Fig. 4D). It is proposed that the combination of these oxides created oxygen deficiencies in the grain boundaries of these catalysts, thus giving rise to improved nitrogen adsorption on these sites. During the reduction, the hematite structure (Fe_2O_3) was

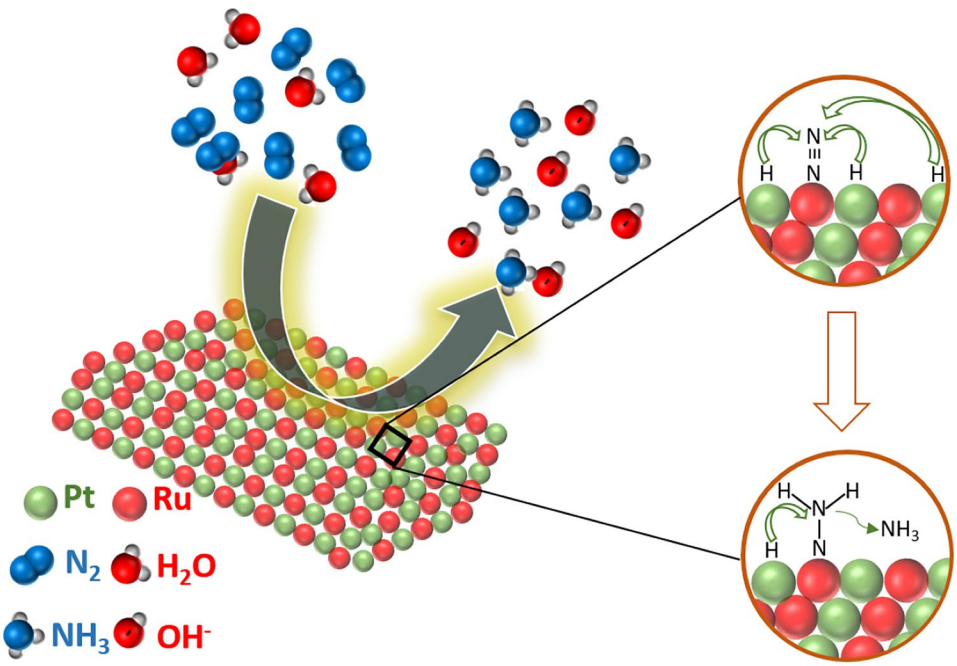

Fig. 3 Schematic representation of the bifunctional activity of the Pt–Ru catalyst system

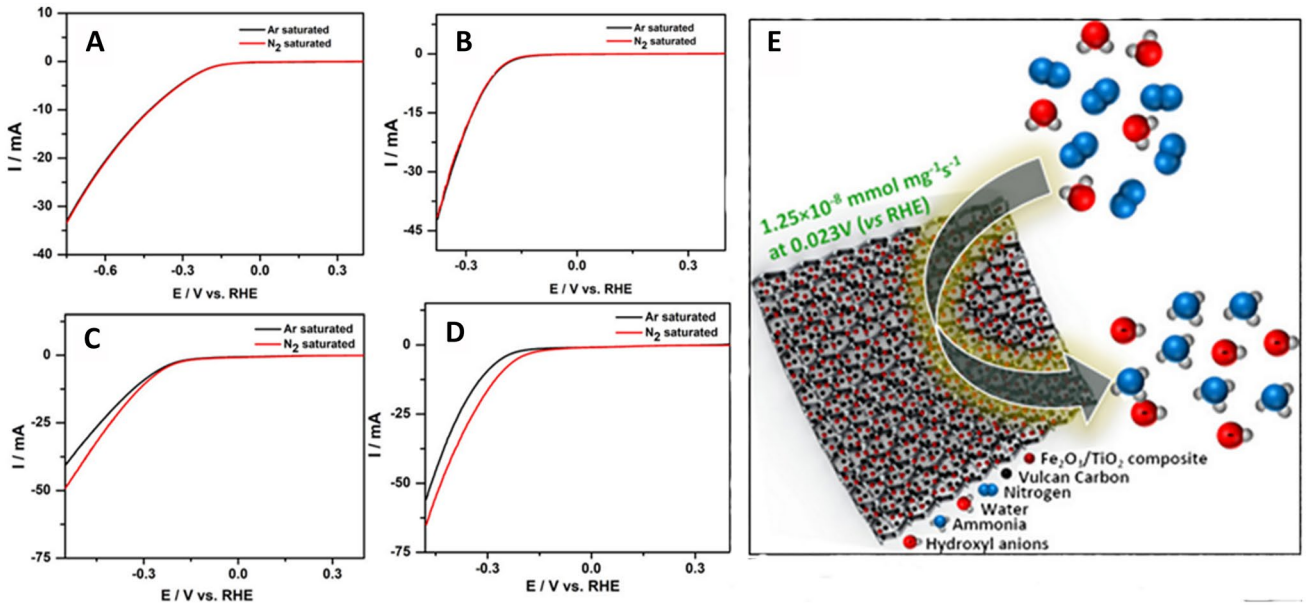

Fig. 4 Linear sweep voltammograms of **A** nickel foam and **B** TiO_2/C-; **C** Fe_2O_3-; and **D** Fe_2O3/TiO_2-coated nickel foam electrodes in an argon-saturated (black curve) and a nitrogen-saturated (red curve) 1.0 M KOH solution. Scan rate 5 mV s^{-1}. **E** Schematic representation of the E-NRR process on the bifunctional Fe_2O_3/TiO_2 catalyst system. Reproduced with permission [111]

partially reduced to magnetite (Fe_3O_4). However, the presence of oxygen in the air preserved the complete reduction of Fe(III) sites and prevented the loss of activity.

In another study, Wang et al. demonstrated the $FeMo_3S_4$ nanorods as an effective and durable electrocatalyst for the nitrogen reduction reaction (NRR) by combined computation and experimental investigations (Fig. 5) [112]. DFT calculations suggested that the 3-fold coordinated Fe (Fe_{3c}) of $FeMo_3S_4$ is the active center for NRR which can efficiently back-donate 3d electrons into the antibonding 1πg* orbital of $*N_2$, to polarize and activate the N_2 molecule, as illustrated in Fig. 5c. This observed activity of $FeMo_3S_4$ correlated with the enzymatic N_2 fixation, where the peripheric Fe−protein around the Fe−Mo−S cofactor serves as a key active site for adsorption and activation of dinitrogen while the Mo−protein plays a secondary role. To understand the role of Mo in $FeMo_3S_4$, the HER activity of $FeMo_3S_4$ was investigated by determining the free energy of absorbed *H (G_{*H}). The results evidenced the G_{*H} of an 8-fold coordinated Mo (Mo_{8c}) site in $FeMo_3S_4$ is much lower in energy (0.54 eV) than that of Fe_{3c} (1.15 eV) (Fig. 5f). This indicates that the Mo_{8c} sites tend to attract protons and thus can help in protecting the NRR-active Fe_{3c} sites from the competing HER reaction. This secondary role of the Mo_{8c} site in $FeMo_3S_4$ is beneficial in achieving the higher FE without disturbing the Fe_{3c} NRR-active sites. The $FeMo_3S_4$ catalyst with bifunctional Fe_{3c} and Mo_{8c} active sites is expected to result in a high NRR activity and selectivity. Consequently, the $FeMo_3S_4$ nanorods exhibited both a high NH_3 yield of 65.3 μg h^{-1} mg^{-1} and a high Faradaic efficiency of 19.2% at − 0.3 V.

Similarly, the bifunctional role of ruthenium–platinum (RuPt) alloy catalyst to electrochemically produce ammonia with high selectivity is reported in our previous study [113]. As shown in Fig. 6B, the ammonia formation rate of 3.0×10^{-10} mol s^{-1} cm^{-2} with a 13.2% FE at an applied potential of 0.123 V vs. RHE and the highest ammonia production rate of 6.37×10^{-10} mol s^{-1} cm^{-2} was achieved at − 0.077 V with a FE of 1.1%. The higher ammonia production rate and excellent FE are attributed to the synergistic mechanism, where the N_2 is adsorbed on a Ru site. At the same time, the preferable formation of Pt-H acts as the hydrogen source, thereby facilitating the selective N_2 activation without disturbing the NRR active Ru site.

Another type of bifunctionality was reported in the study of Zhao et al. which studied the E-NRR activity of [CB[7]-$K_2[B_{12}H_{12}]$@Au] catalyst in which nanogold particles were supported on the dual-functional boron self-assembly carrier CB[7]-$K_2[B_{12}H_{12}]$ [114]. Theoretical calculations revealed that the presence of K^+ ion kinetically suppresses the HER by preventing the H_3O^+ from approaching the gold surface due to the repulsion arising from the positively charged coordination sphere of the K^+ aqua complexes that make it possible to achieve the higher ammonia yield even at higher applied potentials without compromising on the FE. Further, the presence of K^+ lowers the energy of nitrogen reduction to ammonia which was evidenced by Gibbs free energy calculations. Compared to the bare gold, the nitrogen adsorption on K-doped Au (111) is stronger mainly due to the enhanced electron density caused by the charge transfer from K^+ ions to Au (111). This excess surface charge also lowers the free energy of the consecutive steps

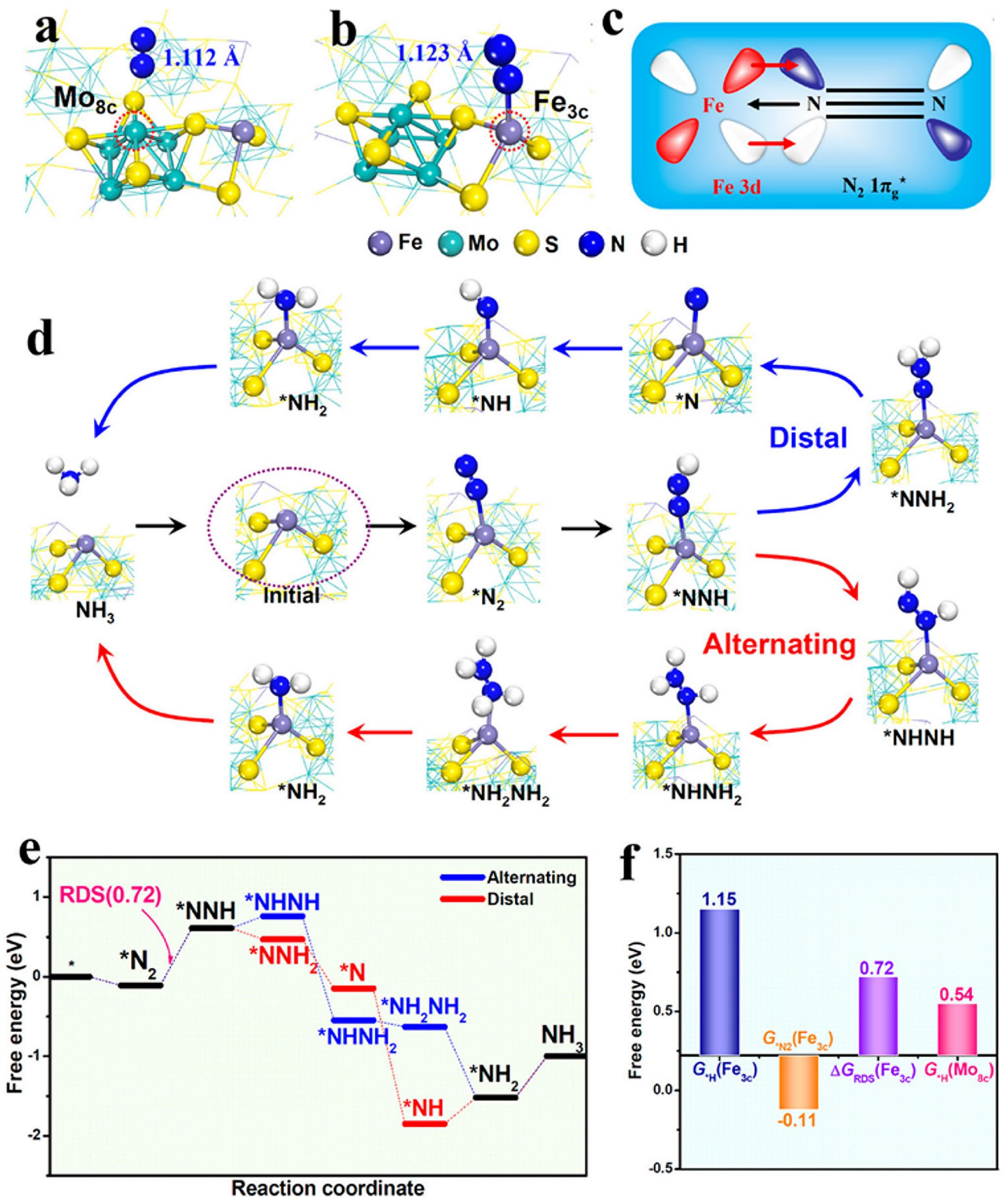

Fig. 5 **a**, **b** Optimized structures of $*N_2$ on **a** Mo8c and **b** Fe3c sites. **c** Schematic of the interaction between Fe atom and *N2. **d** Schematic of the distal and alternating NRR pathways on Fe3c. **e** Gibbs free energy diagrams of NRR pathways on Fe3c at zero potential. **f** Gibbs free energies of *H adsorption on Fe3c (G*H (Fe3c)), *N2 adsorption on Fe3c (G*N2 (Fe3c)), RDS energy barrier on Fe3c (ΔGRDS (Fe3c)), and *H adsorption on Mo8c (G*H (Mo8c)). Reproduced with permission [112]

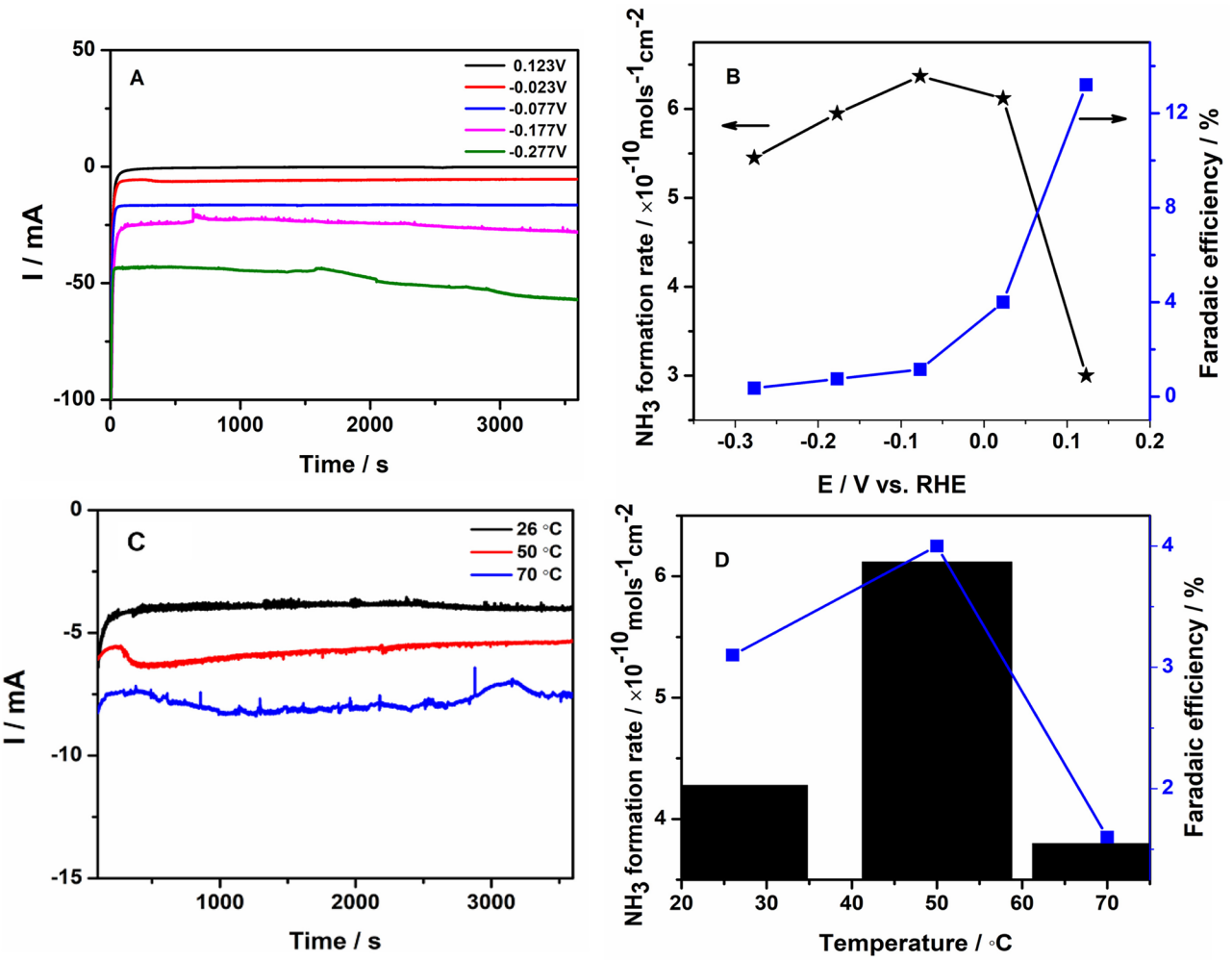

Fig. 6 **A** Chronoamperograms of RuPt/C modified electrodes in 1.0 M KOH under nitrogen atmosphere at various applied potentials. **B** Correlation between rate of ammonia formation and Faradaic efficiency at different potentials. **C** Chronoamperometry of RuPt/C-modified electrodes in 1.0 M KOH under nitrogen atmosphere at different temperatures. **D** Rates of ammonia formation and Faradaic efficiency at various temperatures. Reproduced with permission [113]

by effectively polarizing the nitrogen. Consecutively, the CB[7]-$K_2[B_{12}H_{12}]$@Au electrocatalyst comprising the Au nanoparticles and the K^+ ion that plays a bifunctional role exhibited a higher ammonia yield of 41.69 μg h^{-1} mg_{cat}^{-1} and Faradaic efficiency of 29.53% at − 0.4 V vs RHE. The potential role of the S site in $FeNi_2S_4$/NiS hetero-interface electrocatalysts in inhibiting the occurrence of competing HER on the NRR active Ni site was both experimentally and theoretically studied by Liu et al. [115]. DFT calculations revealed that the barrier for the NNH* formation on the NiS (101) is much lower with a free energy of 0.88 eV than that of both the NiS (102) (0.92eV), and $FeNi_2S_4$ (311) (1.71eV). Further, the DFT calculations disclosed that on all these three structures, HER is more favorable on the top site of the S atom than on the top site of the Ni atom (0.45 vs. 0.95 eV, 0.31 vs. 0.87 eV, and − 0.05 vs. 1.58 eV), and the adsorption energy of N_2 molecule on the top site of Ni atom is more stable than that of the adsorption energy of H atom (0.04 vs. 0.95 eV, 0.22 vs. 0.87 eV, and 0.30 vs. 1.58 eV). These results suggest that E-NRR preferably occurs on the Ni site while the S site protects the NRR active Ni site from the competing HER reaction. Moreover, facile charge transfer resulting from the intimate coupling between the $FeNi_2S_4$ and NiS leads to improved reaction kinetics. As a result, the optimized $FeNi_2S_4$/NiS electrocatalyst (FNS/CC-2) exhibited an ammonia production rate of 128.398 ± 1.32 μg h^{-1} cm^{-2} and a high FE of 28.64 ± 0.18% at − 0.30 V vs. RHE under ambient conditions.

Decreasing the concentration of protons or electrons while increasing the availability of the N_2 is a key strategy in achieving selective ammonia production. This can be achieved via interface engineering of the catalyst with the

aid of a hydrophobic layer. The existence of such a hydrophobic layer suppresses the HER by not only limiting the water concentration but also modifying the d-band center of the TMs; thus, it weakens the H adsorption and preferably adsorbing N_2. For instance, Sim et al. demonstrated the bifunctional role of zeolitic-imidazole framework (ZIF) hydrophobic layer in ZIF modified Pt/Au electrocatalyst [116]. The interface engineering of the ZIF and Pt/Au modify the d-band center of the Pt-Au catalyst thus delivering a FE of > 44% with a high ammonia yield rate of > 161 μg mg_{cat}^{-1} h^{-1} at ambient conditions. As stated above, the ZIF the hydrophobic layer's presence also greatly increases the N_2 concentration and limits the water availability at the electrocatalyst active sites. As a result, the achieved FE with ZIF-coated Pt/Au electrocatalyst is > 44-fold higher compared to the bare Pt/Ru (FE ~ 1%) at a wide range of applied potentials (− 2.1 V to − 2.9 V). Similarly, Xiao modified the self-supporting nanoporous Mo_4P_3 (np-Mo_4P_3) electrode by coating fluoro silane (FAS) to form a hydrophobic surface [117]. This hydrophobic-coated np-Mo_4P_3 catalyst exhibits a FE of 10.1% at − 0.15 V vs. RHE, which is 3.9 times higher than that of the non-coated np-Mo_4P_3 catalyst. Moreover, the hydrophobic np-Mo_4P_3 catalyst exhibits the highest NH_3 yield of ammonia production rate of 17.3 μg h^{-1} cm^{-2}. The key factors, including the d-band center alteration arising from the interaction of FAS and np-Mo_4P_3 thus weakening the H adsorption, and the improved N_2 concentration with limited water concentration near the catalyst center due to the presence of hydrophobic FAS layer, are responsible for this enhanced NRR performance of FAS coated np-Mo_4P_3 electrocatalysts.

In another study, Zhang et al. demonstrated the presence of hydrophobic carbon fiber paper (CFP) on which Au nanoparticles are supported (Au/o-CFP) facilitates the three-phase contact points (TPCPs) for N_2 (gas), electrolyte (liquid), and Au NPs (solid) [118]. Such interfacial engineering improving the N_2 concentration by effectively lowering the proton concentration at the catalyst active sites leads to the higher selectivity for E-NRR over competing HER. Consequently, the Au/o-CFP electrocatalyst with favorable TPCPs exhibited an excellent NRR performance with a high NH_3 yield rate of 40.6 μg h^{-1} mg^{-1} at −0.30 V and maximum FE of 31.3% at − 0.10 V vs. RHE in 0.1 M Na_2SO_4. The role of strong interactions of the hydrophobic interface with N_2 and its weak electrocatalytic activity towards HER was also evidenced from the N_2 bubble contact angle result and cyclic voltammetry analysis. Lai and co-workers enhanced the NRR selectivity of the selenium vacancy-rich $ReSe_2$@carbonized bacterial cellulose (Vr-ReSe2@CBC) nanofiber catalyst by sandwiching it between the two CBC layers [119]. The nitrogen bubble adhesive force analysis, superhydrophilic measurements, and COMSOL Multiphysics simulations demonstrated that the hydrophobic and porous CBC layer prevents the internal Vr-$ReSe_2$@CBC active catalyst layer from water and leads to the more free active sites available for N_2 adsorption and its successive activation. As a result, this unique sandwiched structured catalyst boosted FE by 42.5% and ammonia yield of 28.3 μg h^{-1} cm^{-2} at − 0.25 V. The critical role of the hydrophobic component in elevating the NRR selectivity by suppressing the HER was also studied on several other catalyst systems including the hydrophobic oleylamine-functionalized ZIF-coated Ag-Au [120] and ZIF-coated MoS_2 [121]. As discussed in detail, the coating of the hydrophobic layer mainly leads to the limited availability of water at the active catalyst sites. However, a further study focusing on the restriction of H_3O^+ at the catalyst site is highly required as H_3O^+ acts as the proton donor in the E-NRR process in acidic media [122].

Experimental setup, testing protocols, and various NH_3 quantification methods

The core components for E-NRR study comprise the electrochemical workstation, which includes an electrolytic cell, a working electrode with the catalyst, a reference electrode, and a counter electrode. The choice of the electrolytic cell configuration is important for the nitrogen reduction to ammonia. At present, cell configurations are mainly of four types: (1) back-to-back cells, (2) polymer electrolyte membrane (PEM)-type cells, (3) H-type cells, and (4) single-chamber cells. Figure 7 shows a schematic diagram of the different cell configurations [61, 76]. In back-to-back cells, the E-NRR is mainly performed in the cathode cell, while the anode cell generates O_2 [123, 124]. In addition, the two gas diffusion electrodes are separated by a dense membrane and Nafion membranes which possess high ionic conductivity under ambient conditions [11, 125]. In the PEM-type cell, nitrogen is supplied to the cathodic chamber, and the anode is filled with a liquid electrolyte solution that supplies protons to the cathode by electrolyzing water on the anode. After the reduction, the ammonia gas generated is dissolved in the acidic electrolyte [36]. Here, the cathode has no direct contact with the electrolyte. This type of cell configuration in PEM-type cells and the back-to-back cell helps to inhibit the HER [26, 126, 127]. The H-type cell and single-chamber cell are usually filled with liquid electrolytes. So, there is direct contact between the electrode and the electrolyte [128]. This leads to vast competition between HER and NRR at the catalyst surface and results in a lower rate of NH_3 formation and low Faradaic efficiency [129]. At present, the H-type cell is the most widely used electrolytic cell, where the working and reference electrodes are assembled in the cathode chamber in which the reduction occurs, the counter electrode is located in the anode chamber, and the system allows the precise control of the potential applied to the working electrode. In the

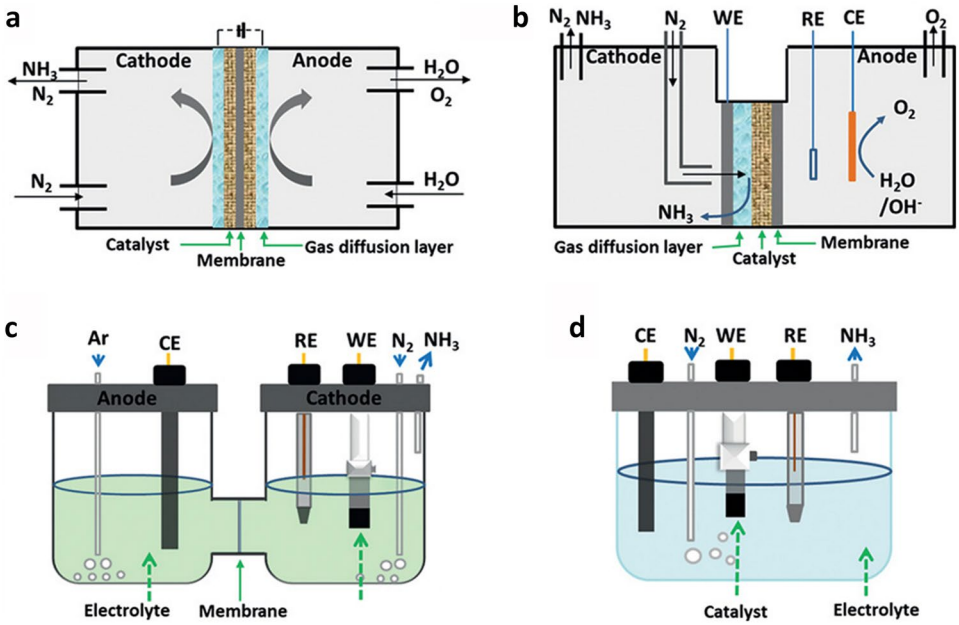

Fig. 7 Schematic view of four different electrocatalytic nitrogen reduction Cell configurations. **a** Back-to-back electrolytic cell, **b** polymer electrolyte membrane (PEM) type electrolytic cell, **c** H-type cell, and **d** single-chamber cell. Reproduced with permission [61]

cases of a single-chamber cell that avoids the use of proton-exchange membranes, the generated NH_3 is easily oxidized to NOx on the anode [130]. Therefore, the use of this cell configuration for the E-NRR is not recommended. In summary, the cell configuration involving two isolated chambers allows more precise and better results for the E-NRR. Another major issue is the solubility of the non-polar N_2 in electrolytes, which is extremely low in most common electrolytes. Researchers found that generally, the use of a flow cell increases the solubility of CO_2 in the electrolyte [61, 131], thereby increasing the current density of the corresponding electrochemical reduction. Hence, it is believed that the use of flow cells can enhance N_2 solubility in the electrolyte by increasing the electrolyte circulation and time of contact between N_2 and hence facilitates the electrocatalytic nitrogen reduction with a better rate of NH_3 formation

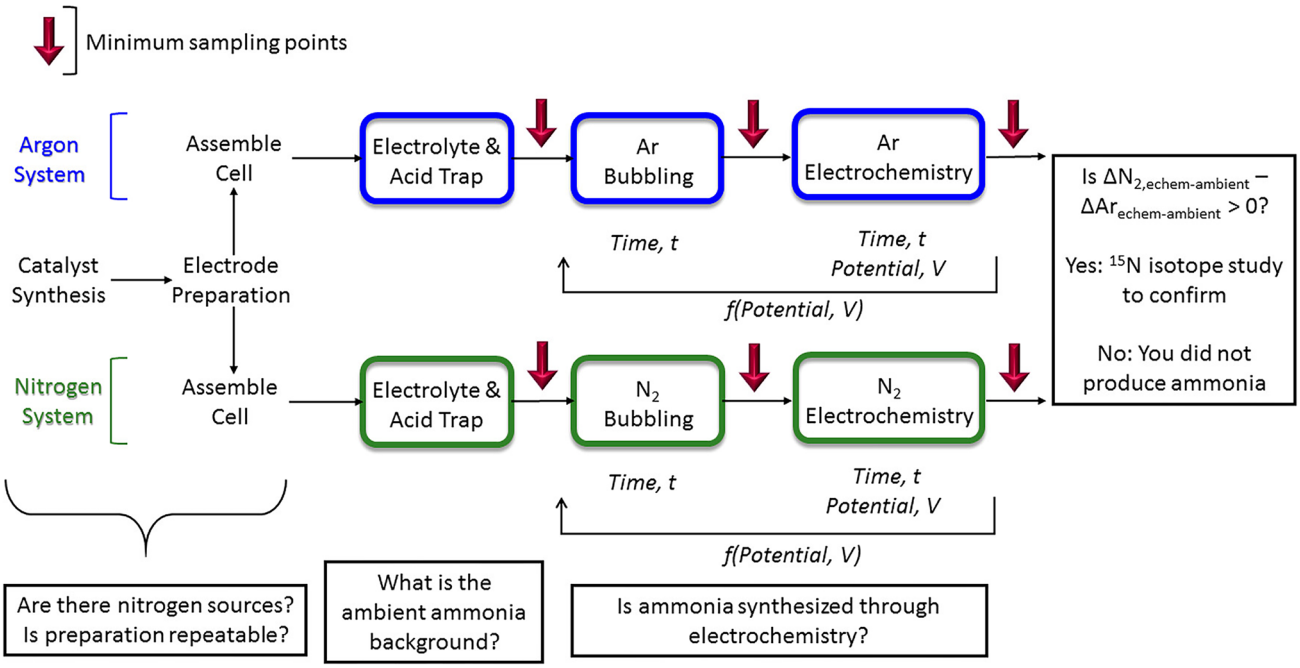

Fig. 8 Flow chart of experimental steps for ENRR and testing protocol. Reproduced with permission [138]

and higher Faradaic efficiency [61]. In E-NRR experiments, the most commonly used counter electrodes are high-purity graphite or Pt. The reference electrode should be selected according to the type of electrode-filling solution, the electrolyte, and the electrode material. In addition, the catalyst is often dispersed on specific support (such as carbon paper, CC, and Ni foam) and fixed on the working electrode. In some reports, the catalyst is directly coated on the working electrode (e.g., glassy carbon) surface. Although this strategy is also suitable for the E-NRR, it should prevent inaccuracies in the normalization of activity caused by the low catalyst loading and ultra-low current density.

Further, selecting a suitable ammonia quantification method is a very critical as well as challenging step which determines the electrocatalytic efficiency of the developed catalysts for the NRR. Hence, the chosen method for ammonia detection must be highly sensitive, selective, accurate, and reproducible. The accurate ammonia quantification methods depend on various parameters such as quantification time, pH, supporting electrolytes, and presence of the scavenging agent. Currently, the NH_3 quantification is mostly accomplished by spectrophotometry or colorimetric methods which include Nessler's reagent, indophenol blue or phenate [132], NH_3-sensitive electrode methods [133], ion chromatography [134], mass spectrometry (MS) [135], ^1H NMR [136], and also some commercially available test kits [26]. In routine experiments, ammonia detection and quantification mostly depend on the indophenol blue method/salicylate method and Nessler's method, due to their good sensitivity, lower detection limit, more stable color development, better reproducibility, and low cost [26, 137–139]. The colorimetric reagent in Nessler's method mainly comprises K_2HgI_4, KOH solution. In an alkaline medium, $[HgI_4]^{2-}$ reacts with NH_3 to form a red-brown complex (Hg_2ONH_2I) with strong absorption at 420 nm which is proportional to the concentration of NH_3 [140]. The indophenol

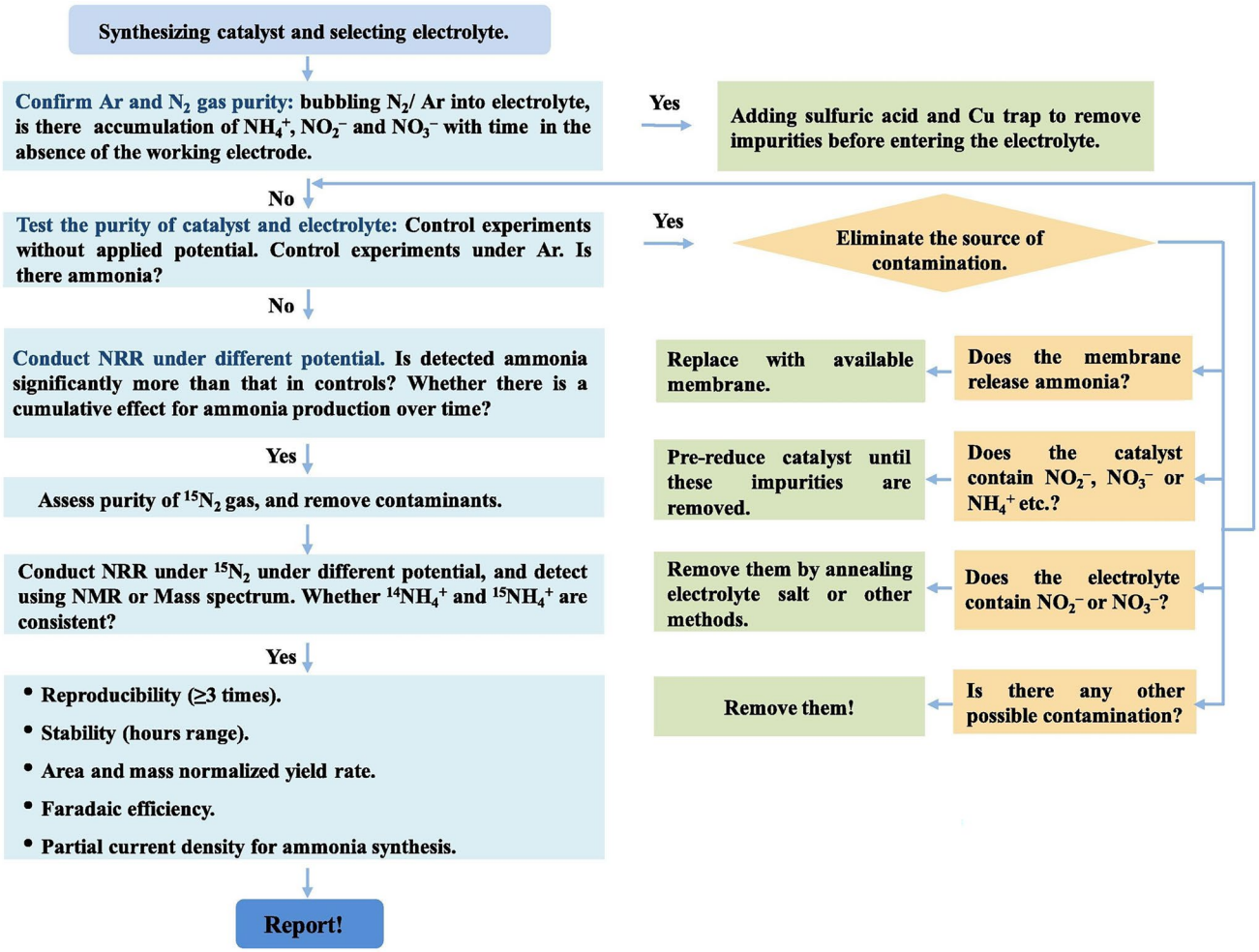

Fig. 9 Summary for determining the E-NRR activity of a catalyst by avoiding the pitfalls in electrocatalytic nitrogen reduction for ammonia synthesis. Reproduced with permission [145]

blue method or the salicylate method comprises sodium nitroprusside dehydrate, salicylic acid, sodium citrate, sodium hypochlorite, and sodium hydroxide. The obtained product in the presence of NH_3 changes its color from light yellow to blue-green depending upon the NH_3 concentration which is linearly related to absorbance at 655 nm [141]. However, these spectrometric methods are closely linked with various parameters such as temperature, time, pH, and reagent concentrations. Hence, control experiments using electrolytes with intentional ion addition are recommended to eliminate the potential interferences [132, 142]. Excellent reproducibility and accuracy are obtained by the well-known ion chromatography technique which uses the principle of ion exchange to determine specific ionic strength. Suitable ion-exchange columns such as Dionex IonPac CS16-4 mm Column, Origin 9512HPBNWP NH_3, and Radiometer Analytical ISE25NH4-9 NH_4^+ can reliably quantify NH_4^+ ions with a low detection limit and larger detection range (5×10^{-7} or 3×10^{-6} mol L^{-1}). However, this method requires a much longer measurement time to attain stable and precise results at lower concentrations, and it is not suitable for organic electrolytes as well as electrolytes containing Li^+ and Na^+ due to the shorter retention time [26, 112, 143]. ^1H NMR can be used to analyze NH_3 present in the electrolyte both quantitatively and qualitatively and has excellent resolution for $^{14}NH_4^+$ and $^{15}NH_4^+$ [136, 144]. In mass spectrometry, $^{14}NH_4^+$ and $^{15}NH_4^+$ can be differentiated based on their mass/charge ratio (m/z), and quantitative measurements can be performed using the relationship between the mass spectrometric signal and analyte amount. In ^1H NMR, $^{14}NH_4^+$ affords three peaks of equal intensity, while the signal of $^{15}NH_4^+$ is split into two peaks of equal intensity, which allows one to distinguish these ions. Moreover, NH_3 can be quantified using integrated peak areas [145]. It is highly important to note that the NMR isotope labeling method is costly and insensitive to very low concentrations. Therefore, it is not suitable for every measurement and should be applied only for catalysts that contain nitrogen in their structure (e.g., metal nitrides, nitrogen-doped carbon, and nitrogen coordinated metal complexes) to quantify the electrochemically formed from the leached out ammonia. The background ammonia signal can be easily subtracted from the sample in metal and metal oxide electrodes. Finally, to avoid false results, it is recommended to run NRR experiments rigorously by performing a set of non-electrochemical and electrochemical experiments in both Ar and N_2 for each catalyst to verify that the ammonia measurements are repeatable and reliable. A general sequence for electrochemically formed ammonia detection and quantification is shown in Fig. 8, and the systematic evaluation of the E-NRR activity avoiding the pitfalls is exemplified in Fig. 9.

Summary comprising the possible research directions and future perspectives

In this review, we have attempted to summarize the recent development of the electrocatalysts including the catalysts that play a bifunctional role in effectively addressing the limitation associated with the electrochemical ammonia synthesis under ambient conditions. Understanding the reaction mechanism is the key challenge of the E-NRR process from the theoretical prediction of suitable electrocatalysts to cell design and ammonia quantification methods; all these were concisely highlighted. Designing strategies implemented in the featured studies summarized in this review, particularly the designing strategy of bifunctional catalysts, can be extended to create a series of such bifunctional activity materials in view of further improving the performance art ambient condition electrochemical ammonia synthesis. Particularly, the future study focusing on the role of secondary hydrophobic coating in restricting the H_3O^+ at the catalyst site is highly required to realize higher E-NRR selectivity in acidic media as H_3O^+ acts as the proton donor into the adsorbed $*N_xH_y$ intermediates (x = 1–2, y = 0–5) process in this media. Catalysts with high-affinity active sites to protons adjacent to the NRR active sites may also have higher NRR activity.

Another approach would be the development of non-aqueous or low free water-electrolyte solutions, which will have high N_2 solubility and low HER kinetics (high overpotential), thus enabling a wider electrochemical potential window for NRR without the hindrance of competing reactions. Fast-growing research in the E-NRR field is highly promising for renewable energy storage on a large scale and holds great potential for improvement from its current performance level, which can be realized by an innovative approach relying on a fundamental understanding of the electrocatalytic reaction on various materials surfaces.

Supplementary information The online version contains supplementary material available at https://doi.org/10.1007/s10008-022-05228-5.

References

1. Zakzeski J, Bruijnincx PCA, Jongerius AL, Weckhuysen BM (2010) The catalytic valorization of lignin for the production of renewable chemicals. Chem Rev 110:3552–3599. https://doi.org/10.1021/cr900354u
2. Panda R, Maity M (2021) Global warming and climate change on earth: duties and challenges of human beings. Int J Res Eng Sci Manag 4:122–125
3. Li Y, Wang H, Priest C et al (2021) Advanced electrocatalysis for energy and environmental sustainability via water and nitrogen reactions. Adv Mater 33:2000381. https://doi.org/10.1002/adma.202000381

4. Qing G, Ghazfar R, Jackowski ST et al (2020) Recent advances and challenges of electrocatalytic N2 reduction to ammonia. Chem Rev 120:5437–5516. https://doi.org/10.1021/acs.chemrev.9b00659
5. Li W, Fang W, Wu C et al (2020) Bimetal–MOF nanosheets as efficient bifunctional electrocatalysts for oxygen evolution and nitrogen reduction reaction. J Mater Chem A 8:3658–3666. https://doi.org/10.1039/C9TA13473E
6. He Y, Tan Q, Lu L et al (2019) Metal-nitrogen-carbon catalysts for oxygen reduction in PEM fuel cells: self-template synthesis approach to enhancing catalytic activity and stability. Electrochem Energy Rev 2:231–251. https://doi.org/10.1007/s41918-019-00031-9
7. Manjunatha R, Karajić A, Liu M et al (2020) A review of composite/hybrid electrocatalysts and photocatalysts for nitrogen reduction reactions: advanced materials, mechanisms, challenges and perspectives. Electrochem Energy Rev 3:506–540. https://doi.org/10.1007/s41918-020-00069-0
8. Ghavam S, Vahdati M, Wilson IAG, Styring P (2021) Sustainable ammonia production processes. Front Energy Res 9
9. Hanada N, Hino S, Ichikawa T et al (2010) Hydrogen generation by electrolysis of liquid ammonia. Chem Commun 46:7775–7777. https://doi.org/10.1039/C0CC01982H
10. Erisman JW, Sutton MA, Galloway J et al (2008) How a century of ammonia synthesis changed the world. Nat Geosci 1:636–639. https://doi.org/10.1038/ngeo325
11. Amar IA, Lan R, Petit CTG, Tao S (2011) Solid-state electrochemical synthesis of ammonia: a review. J Solid State Electrochem 15:1845. https://doi.org/10.1007/s10008-011-1376-x
12. Smil V (2000) Enriching the Earth: Fritz Haber, Carl Bosch, and the transformation of world food production
13. Dunikowska M, Turko L (2011) Fritz Haber: the damned scientist. Angew Chemie Int Ed 50:10050–10062. https://doi.org/10.1002/anie.201105425
14. Brightling J (2018) Ammonia and the fertiliser industry: the development of ammonia at Billingham. Johnson Matthey Technol Rev 62:32–47. https://doi.org/10.1595/205651318X696341
15. Montoya JH, Tsai C, Vojvodic A, Nørskov JK (2015) The challenge of electrochemical ammonia synthesis: a new perspective on the role of nitrogen scaling relations. Chem Sus Chem 8:2180–2186. https://doi.org/10.1002/cssc.201500322
16. Lipman T, Shah N (2007) Ammonia as an alternative energy storage medium for hydrogen fuel cells. Escholarsh Repos Univ Calif
17. Foster SL, Bakovic SIP, Duda RD et al (2018) Catalysts for nitrogen reduction to ammonia. Nat Catal 1:490–500. https://doi.org/10.1038/s41929-018-0092-7
18. Martín AJ, Shinagawa T, Pérez-Ramírez J (2019) Electrocatalytic reduction of nitrogen: from Haber-Bosch to ammonia artificial leaf. Chem 5:263–283. https://doi.org/10.1016/j.chempr.2018.10.010
19. Kyriakou V, Garagounis I, Vourros A et al (2020) An electrochemical Haber-Bosch process. Joule 4:142–158. https://doi.org/10.1016/j.joule.2019.10.006
20. Bertilsson GOB, Kirchmann H (2021) Sustainable N fertilizer production based on a loop: straw-biogas-'Haber-Bosch' process. Agric Syst 190:103100. https://doi.org/10.1016/j.agsy.2021.103100
21. Xu G-R, Batmunkh M, Donne S et al (2019) Ruthenium(iii) polyethyleneimine complexes for bifunctional ammonia production and biomass upgrading. J Mater Chem A 7:25433–25440. https://doi.org/10.1039/C9TA10267A
22. Liu H, Wei L, Liu F et al (2019) Homogeneous, heterogeneous, and biological catalysts for electrochemical N2 reduction toward NH3 under ambient conditions. ACS Catal 9:5245–5267. https://doi.org/10.1021/acscatal.9b00994
23. Li M, Huang H, Low J et al (2019) Recent progress on electrocatalyst and photocatalyst design for nitrogen reduction. Small Methods 3:1800388. https://doi.org/10.1002/smtd.201800388
24. Cui X, Tang C, Zhang Q (2018) A review of electrocatalytic reduction of dinitrogen to ammonia under ambient conditions. Adv Energy Mater 8:1800369. https://doi.org/10.1002/aenm.201800369
25. Lv C, Yan C, Chen G et al (2018) An amorphous noble-metal-free electrocatalyst that enables nitrogen fixation under ambient conditions. Angew Chemie Int Ed 57:6073–6076. https://doi.org/10.1002/anie.201801538
26. Chen G-F, Yuan Y, Jiang H et al (2020) Electrochemical reduction of nitrate to ammonia via direct eight-electron transfer using a copper–molecular solid catalyst. Nat Energy 5:605–613. https://doi.org/10.1038/s41560-020-0654-1
27. Li J, Zhan G, Yang J et al (2020) Efficient ammonia electrosynthesis from nitrate on strained ruthenium nanoclusters. J Am Chem Soc 142:7036–7046. https://doi.org/10.1021/jacs.0c00418
28. Zhang G, Sewell CD, Zhang P et al (2020) Nanostructured photocatalysts for nitrogen fixation. Nano Energy 71:104645. https://doi.org/10.1016/j.nanoen.2020.104645
29. Rouwenhorst KHR, Engelmann Y, van't Veer K et al (2020) Plasma-driven catalysis: green ammonia synthesis with intermittent electricity. Green Chem 22:6258–6287. https://doi.org/10.1039/D0GC02058C
30. Burris RH, Roberts GP (1993) Biological nitrogen fixation. Annu Rev Nutr 13:317–335. https://doi.org/10.1146/annurev.nu.13.070193.001533
31. Chen X, Guo Y, Du X et al (2020) Atomic structure modification for electrochemical nitrogen reduction to ammonia. Adv Energy Mater 10:1903172. https://doi.org/10.1002/aenm.201903172
32. Huang H, Gong F, Wang Y et al (2019) Mn3O4 nanoparticles@reduced graphene oxide composite: an efficient electrocatalyst for artificial N2 fixation to NH3 at ambient conditions. Nano Res 12:1093–1098. https://doi.org/10.1007/s12274-019-2352-5
33. Singh AR, Rohr BA, Schwalbe JA et al (2017) Electrochemical ammonia synthesis—the selectivity challenge. ACS Catal 7:706–709. https://doi.org/10.1021/acscatal.6b03035
34. Wang P, Chang F, Gao W et al (2017) Breaking scaling relations to achieve low-temperature ammonia synthesis through LiH-mediated nitrogen transfer and hydrogenation. Nat Chem 9:64–70. https://doi.org/10.1038/nchem.2595
35. Juangsa FB, Irhamna AR, Aziz M (2021) Production of ammonia as potential hydrogen carrier: review on thermochemical and electrochemical processes. Int J Hydrogen Energy 46:14455–14477. https://doi.org/10.1016/j.ijhydene.2021.01.214
36. Kordali V, Kyriacou G, Lambrou C (2000) Electrochemical synthesis of ammonia at atmospheric pressure and low temperature in a solid polymer electrolyte cell. Chem Commun. https://doi.org/10.1039/B004885M
37. Jia H-P, Quadrelli EA (2014) Mechanistic aspects of dinitrogen cleavage and hydrogenation to produce ammonia in catalysis and organometallic chemistry: relevance of metal hydride bonds and dihydrogen. Chem Soc Rev 43:547–564. https://doi.org/10.1039/C3CS60206K
38. van der Ham CJM, Koper MTM, Hetterscheid DGH (2014) Challenges in reduction of dinitrogen by proton and electron transfer. Chem Soc Rev 43:5183–5191. https://doi.org/10.1039/C4CS00085D
39. Wang H, Chen Y, Fan R et al (2019) Selective electrochemical reduction of nitrogen to ammonia by adjusting the three-phase interface. Research 2019:1401209. https://doi.org/10.34133/2019/1401209
40. Hou J, Yang M, Zhang J (2020) Recent advances in catalysts, electrolytes and electrode engineering for the nitrogen reduction reaction under ambient conditions. Nanoscale 12:6900–6920. https://doi.org/10.1039/D0NR00412J

41. Skúlason E, Bligaard T, Gudmundsdóttir S et al (2012) A theoretical evaluation of possible transition metal electro-catalysts for N2 reduction. Phys Chem Chem Phys 14:1235–1245. https://doi.org/10.1039/C1CP22271F
42. Chen G-F, Cao X, Wu S et al (2017) Ammonia electrosynthesis with high selectivity under ambient conditions via a Li+ incorporation strategy. J Am Chem Soc 139:9771–9774. https://doi.org/10.1021/jacs.7b04393
43. Chen JG, Crooks RM, Seefeldt LC et al (2018) Beyond fossil fuel–driven nitrogen transformations. Science (80-) 360:eaar6611. https://doi.org/10.1126/science.aar6611
44. Tang C, Qiao S-Z (2019) How to explore ambient electrocatalytic nitrogen reduction reliably and insightfully. Chem Soc Rev 48:3166–3180. https://doi.org/10.1039/C9CS00280D
45. Bezdek MJ, Chirik PJ (2018) Interconversion of molybdenum imido and amido complexes by proton-coupled electron transfer. Angew Chemie Int Ed 57:2224–2228. https://doi.org/10.1002/anie.201708406
46. Lv C, Zhong L, Yao Y et al (2020) Boosting electrocatalytic ammonia production through mimicking "π back-donation." Chem 6:2690–2702. https://doi.org/10.1016/j.chempr.2020.07.006
47. Jiao Y, Zheng Y, Davey K, Qiao S-Z (2016) Activity origin and catalyst design principles for electrocatalytic hydrogen evolution on heteroatom-doped graphene. Nat Energy 1:16130. https://doi.org/10.1038/nenergy.2016.130
48. Guo C, Ran J, Vasileff A, Qiao S-Z (2018) Rational design of electrocatalysts and photo(electro)catalysts for nitrogen reduction to ammonia (NH3) under ambient conditions. Energy Environ Sci 11:45–56. https://doi.org/10.1039/C7EE02220D
49. Giddey S, Badwal SPS, Kulkarni A (2013) Review of electrochemical ammonia production technologies and materials. Int J Hydrogen Energy 38:14576–14594. https://doi.org/10.1016/j.ijhydene.2013.09.054
50. Shilov AE (2003) Catalytic reduction of molecular nitrogen in solutions. Russ Chem Bull 52:2555–2562. https://doi.org/10.1023/B:RUCB.0000019873.81002.60
51. Bazhenova TA, Shilov AE (1995) Nitrogen fixation in solution. Coord Chem Rev 144:69–145. https://doi.org/10.1016/0010-8545(95)01139-G
52. Liu D, Chen M, Du X et al (2021) Development of electrocatalysts for efficient nitrogen reduction reaction under ambient condition. Adv Funct Mater 31:2008983. https://doi.org/10.1002/adfm.202008983
53. Deng J, Iñiguez JA, Liu C (2018) Electrocatalytic nitrogen reduction at low temperature. Joule 2:846–856. https://doi.org/10.1016/j.joule.2018.04.014
54. John J, Lee D-K, Sim U (2019) Photocatalytic and electrocatalytic approaches towards atmospheric nitrogen reduction to ammonia under ambient conditions. Nano Converg 6:15. https://doi.org/10.1186/s40580-019-0182-5
55. Chanda D, Xing R, Xu T et al (2021) Electrochemical nitrogen reduction: recent progress and prospects. Chem Commun 57:7335–7349. https://doi.org/10.1039/D1CC01451J
56. MacLeod KC, Holland PL (2013) Recent developments in the homogeneous reduction of dinitrogen by molybdenum and iron. Nat Chem 5:559–565. https://doi.org/10.1038/nchem.1620
57. Zeinalipour-Yazdi CD, Hargreaves JSJ, Catlow CRA (2015) Nitrogen activation in a Mars–van Krevelen mechanism for ammonia synthesis on Co3Mo3N. J Phys Chem C 119:28368–28376. https://doi.org/10.1021/acs.jpcc.5b06811
58. Anderson JS, Cutsail GE, Rittle J et al (2015) Characterization of an Fe≡N–NH2 intermediate relevant to catalytic N2 reduction to NH3. J Am Chem Soc 137:7803–7809. https://doi.org/10.1021/jacs.5b03432
59. Abghoui Y, Skúlason E (2017) Onset potentials for different reaction mechanisms of nitrogen activation to ammonia on transition metal nitride electro-catalysts. Catal Today 286:69–77. https://doi.org/10.1016/j.cattod.2016.11.047
60. Göttle AJ, Koper MTM (2017) Proton-coupled electron transfer in the electrocatalysis of CO2 reduction: prediction of sequential vs. concerted pathways using DFT. Chem Sci 8:458–465. https://doi.org/10.1039/C6SC02984A
61. Zhao X, Hu G, Chen G-F et al (2021) Comprehensive understanding of the thriving ambient electrochemical nitrogen reduction reaction. Adv Mater 33:2007650. https://doi.org/10.1002/adma.202007650
62. Kumar CVS, Subramanian V (2017) Can boron antisites of BNNTs be an efficient metal-free catalyst for nitrogen fixation? A DFT investigation. Phys Chem Chem Phys 19:15377–15387. https://doi.org/10.1039/C7CP02220D
63. Song R, Yang J, Wang M et al (2021) Theoretical study on P-coordinated metal atoms embedded in arsenene for the conversion of nitrogen to ammonia. ACS Omega 6:8662–8671. https://doi.org/10.1021/acsomega.1c00581
64. Luo H, Wang X, Wan C et al (2022) A theoretical study of Fe adsorbed on pure and nonmetal (N, F, P, S, Cl)-doped Ti3C2O2 for electrocatalytic nitrogen reduction. Nanomater 12
65. Jiao L, Guo L (2022) Theoretical study on the efficient electrocatalytic N2 reduction reaction of bimetallic single atom embedded in phthalocyanine. SSRN Electron J. https://doi.org/10.2139/ssrn.4055255
66. Höskuldsson ÁB, Abghoui Y, Gunnarsdóttir AB, Skúlason E (2017) Computational screening of rutile oxides for electrochemical ammonia formation. ACS Sustain Chem Eng 5:10327–10333. https://doi.org/10.1021/acssuschemeng.7b02379
67. Abghoui Y, Skúlason E (2017) Electrochemical synthesis of ammonia via Mars-van Krevelen mechanism on the (111) facets of group III–VII transition metal mononitrides. Catal Today 286:78–84. https://doi.org/10.1016/j.cattod.2016.06.009
68. Li Q, Liu C, Qiu S et al (2019) Exploration of iron borides as electrochemical catalysts for the nitrogen reduction reaction. J Mater Chem A 7:21507–21513. https://doi.org/10.1039/C9TA04650J
69. Jasin Arachchige L, Xu Y, Dai Z et al (2020) Theoretical investigation of single and double transition metals anchored on graphyne monolayer for nitrogen reduction reaction. J Phys Chem C 124:15295–15301. https://doi.org/10.1021/acs.jpcc.0c03899
70. Xu Y, Cai Z, Du P et al (2021) Taming the challenges of activity and selectivity in the electrochemical nitrogen reduction reaction using graphdiyne-supported double-atom catalysts. J Mater Chem A 9:8489–8500. https://doi.org/10.1039/D1TA00262G
71. Zhai X, Li L, Liu X et al (2020) A DFT screening of single transition atoms supported on MoS2 as highly efficient electrocatalysts for the nitrogen reduction reaction. Nanoscale 12:10035–10043. https://doi.org/10.1039/D0NR00030B
72. Li L, Wang X, Guo H et al (2019) Theoretical screening of single transition metal atoms embedded in MXene defects as superior electrocatalyst of nitrogen reduction reaction. Small Methods 3:1900337. https://doi.org/10.1002/smtd.201900337
73. Lv X, Wei W, Huang B et al (2021) High-throughput screening of synergistic transition metal dual-atom catalysts for efficient nitrogen fixation. Nano Lett 21:1871–1878. https://doi.org/10.1021/acs.nanolett.0c05080
74. Kong X, Peng H-Q, Bu S et al (2020) Defect engineering of nanostructured electrocatalysts for enhancing nitrogen reduction. J Mater Chem A 8:7457–7473. https://doi.org/10.1039/D0TA01453B
75. Zhao T, Tian Y, Yan L, Su Z (2022) Metal-free C5N2 doped with a boron atom as an efficient electrocatalyst for the nitrogen reduction reaction. New J Chem 46:2282–2289. https://doi.org/10.1039/D1NJ04909G

76. Wang J, Chen S, Li Z et al (2020) Recent advances in electrochemical synthesis of ammonia through nitrogen reduction under ambient conditions. Chem Electro Chem 7:1067–1079. https://doi.org/10.1002/celc.201901967
77. Hao R, Sun W, Liu Q et al (2020) Efficient electrochemical nitrogen fixation over isolated Pt sites. Small 16:2000015. https://doi.org/10.1002/smll.202000015
78. Cao Y, Gao Y, Zhou H et al (2018) Highly efficient ammonia synthesis electrocatalyst: single Ru atom on naturally nanoporous carbon materials. Adv Theory Simulations 1:1800018. https://doi.org/10.1002/adts.201800018
79. Lin B, Heng L, Fang B et al (2019) Ammonia synthesis activity of alumina-supported ruthenium catalyst enhanced by alumina phase transformation. ACS Catal 9:1635–1644. https://doi.org/10.1021/acscatal.8b03554
80. Liu H-M, Han S-H, Zhao Y et al (2018) Surfactant-free atomically ultrathin rhodium nanosheet nanoassemblies for efficient nitrogen electroreduction. J Mater Chem A 6:3211–3217. https://doi.org/10.1039/C7TA10866D
81. Bao D, Zhang Q, Meng F-L et al (2017) Electrochemical reduction of N2 under ambient conditions for artificial N2 fixation and renewable energy storage using N2/NH3 cycle. Adv Mater 29:1604799. https://doi.org/10.1002/adma.201604799
82. Wang Z, Li Y, Yu H et al (2018) Ambient electrochemical synthesis of ammonia from nitrogen and water catalyzed by flower-like gold microstructures. Chem Sus Chem 11:3480–3485. https://doi.org/10.1002/cssc.201801444
83. Shi M-M, Bao D, Li S-J et al (2018) Anchoring PdCu amorphous nanocluster on graphene for electrochemical reduction of N2 to NH3 under ambient conditions in aqueous solution. Adv Energy Mater 8:1800124. https://doi.org/10.1002/aenm.201800124
84. Nazemi M, Panikkanvalappil SR, El-Sayed MA (2018) Enhancing the rate of electrochemical nitrogen reduction reaction for ammonia synthesis under ambient conditions using hollow gold nanocages. Nano Energy 49:316–323. https://doi.org/10.1016/j.nanoen.2018.04.039
85. Wang H, Yu H, Wang Z et al (2019) Electrochemical fabrication of porous Au film on Ni foam for nitrogen reduction to ammonia. Small 15:1804769. https://doi.org/10.1002/smll.201804769
86. Back S, Jung Y (2016) On the mechanism of electrochemical ammonia synthesis on the Ru catalyst. Phys Chem Chem Phys 18:9161–9166. https://doi.org/10.1039/C5CP07363D
87. Wang D, Azofra LM, Harb M et al (2018) Energy-efficient nitrogen reduction to ammonia at low overpotential in aqueous electrolyte under ambient conditions. Chem Sus Chem 11:3416–3422. https://doi.org/10.1002/cssc.201801632
88. Geng Z, Liu Y, Kong X et al (2018) Achieving a record-high yield rate of 120.9 for N2 electrochemical reduction over Ru single-atom catalysts. Adv Mater 30:1803498. https://doi.org/10.1002/adma.201803498
89. Wang J, Yu L, Hu L et al (2018) Ambient ammonia synthesis via palladium-catalyzed electrohydrogenation of dinitrogen at low overpotential. Nat Commun 9:1795. https://doi.org/10.1038/s41467-018-04213-9
90. Morales-Guio CG, Stern L-A, Hu X (2014) Nanostructured hydrotreating catalysts for electrochemical hydrogen evolution. Chem Soc Rev 43:6555–6569. https://doi.org/10.1039/C3CS60468C
91. Qin G, Cui Q, Du A et al (2019) Transition metal diborides: a new type of high-performance electrocatalysts for nitrogen reduction. Chem Cat Chem 11:2624–2633. https://doi.org/10.1002/cctc.201900538
92. Marc-André L, Guillaume B-C, Dewhurst RD et al (2018) Nitrogen fixation and reduction at boron. Science (80-) 359:896–900. https://doi.org/10.1126/science.aaq1684
93. Rostamikia G, Maheshwari S, Janik MJ (2019) Elementary kinetics of nitrogen electroreduction to ammonia on late transition metals. Catal Sci Technol 9:174–181. https://doi.org/10.1039/C8CY01845F
94. Burgess BK, Lowe DJ (1996) Mechanism of molybdenum nitrogenase. Chem Rev 96:2983–3012. https://doi.org/10.1021/cr950055x
95. Eady RR (1996) Structure−function relationships of alternative nitrogenases. Chem Rev 96:3013–3030. https://doi.org/10.1021/cr950057h
96. Zhang L, Ji X, Ren X et al (2018) Electrochemical ammonia synthesis via nitrogen reduction reaction on a MoS2 catalyst: theoretical and experimental studies. Adv Mater 30:1800191. https://doi.org/10.1002/adma.201800191
97. Yang D, Chen T, Wang Z (2017) Electrochemical reduction of aqueous nitrogen (N2) at a low overpotential on (110)-oriented Mo nanofilm. J Mater Chem A 5:18967–18971. https://doi.org/10.1039/C7TA06139K
98. Zhou F, Azofra LM, Ali M et al (2017) Electro-synthesis of ammonia from nitrogen at ambient temperature and pressure in ionic liquids. Energy Environ Sci 10:2516–2520. https://doi.org/10.1039/C7EE02716H
99. Huang L, Wu J, Han P et al (2019) NbO2 electrocatalyst toward 32% Faradaic efficiency for N2 fixation. Small Methods 3:1800386. https://doi.org/10.1002/smtd.201800386
100. Han J, Liu Z, Ma Y et al (2018) Ambient N2 fixation to NH3 at ambient conditions: using Nb2O5 nanofiber as a high-performance electrocatalyst. Nano Energy 52:264–270. https://doi.org/10.1016/j.nanoen.2018.07.045
101. Kong J, Lim A, Yoon C et al (2017) Electrochemical synthesis of NH3 at low temperature and atmospheric pressure using a γ-Fe2O3 catalyst. ACS Sustain Chem Eng 5:10986–10995. https://doi.org/10.1021/acssuschemeng.7b02890
102. Abghoui Y, Garden AL, Hlynsson VF et al (2015) Enabling electrochemical reduction of nitrogen to ammonia at ambient conditions through rational catalyst design. Phys Chem Chem Phys 17:4909–4918. https://doi.org/10.1039/C4CP04838E
103. Zhang R, Zhang Y, Ren X et al (2018) High-efficiency electrosynthesis of ammonia with high selectivity under ambient conditions enabled by VN nanosheet array. ACS Sustain Chem Eng 6:9545–9549. https://doi.org/10.1021/acssuschemeng.8b01261
104. Li Q, He L, Sun C, Zhang X (2017) Computational study of MoN2 monolayer as electrochemical catalysts for nitrogen reduction. J Phys Chem C 121:27563–27568. https://doi.org/10.1021/acs.jpcc.7b10522
105. Manjunatha R, Karajić A, Teller H et al (2020) Electrochemical and chemical instability of vanadium nitride in the synthesis of ammonia directly from nitrogen. Chem Cat Chem 12:438–443. https://doi.org/10.1002/cctc.201901558
106. Zhang L-H, Yu F, Shiju NR (2021) Carbon-based catalysts for selective electrochemical nitrogen-to-ammonia conversion. ACS Sustain Chem Eng 9:7687–7703. https://doi.org/10.1021/acssuschemeng.1c00575
107. Li W, Wu T, Zhang S et al (2018) Nitrogen-free commercial carbon cloth with rich defects for electrocatalytic ammonia synthesis under ambient conditions. Chem Commun 54:11188–11191. https://doi.org/10.1039/C8CC06000B
108. Lv C, Qian Y, Yan C et al (2018) Defect engineering metal-free polymeric carbon nitride electrocatalyst for effective nitrogen fixation under ambient conditions. Angew Chemie Int Ed 57:10246–10250. https://doi.org/10.1002/anie.201806386
109. Hu C, Dai L (2017) Multifunctional carbon-based metal-free electrocatalysts for simultaneous oxygen reduction, oxygen evolution, and hydrogen evolution. Adv Mater 29:1604942. https://doi.org/10.1002/adma.201604942

110. Lv J, Wu S, Tian Z et al (2019) Construction of PdO–Pd interfaces assisted by laser irradiation for enhanced electrocatalytic N2 reduction reaction. J Mater Chem A 7:12627–12634. https://doi.org/10.1039/C9TA02045D
111. Manjunatha R, Karajić A, Goldstein V, Schechter A (2019) Electrochemical ammonia generation directly from nitrogen and air using an iron-oxide/titania-based catalyst at ambient conditions. ACS Appl Mater Interfaces 11:7981–7989. https://doi.org/10.1021/acsami.8b20692
112. Wang J, Nan H, Tian Y, Chu K (2020) FeMo3S4 for efficient nitrogen reduction reaction. ACS Sustain Chem Eng 8:12733–12740. https://doi.org/10.1021/acssuschemeng.0c04091
113. Manjunatha R, Schechter A (2018) Electrochemical synthesis of ammonia using ruthenium–platinum alloy at ambient pressure and low temperature. Electrochem Commun 90:96–100. https://doi.org/10.1016/j.elecom.2018.04.008
114. Zhao X, Yang Z, Kuklin AV et al (2020) Potassium ions promote electrochemical nitrogen reduction on nano-Au catalysts triggered by bifunctional boron supramolecular assembly. J Mater Chem A 8:13086–13094. https://doi.org/10.1039/D0TA04580B
115. Liu P-Y, Shi K, Chen W-Z et al (2021) Enhanced electrocatalytic nitrogen reduction reaction performance by interfacial engineering of MOF-based sulfides FeNi2S4/NiS hetero-interface. Appl Catal B Environ 287:119956. https://doi.org/10.1016/j.apcatb.2021.119956
116. Sim HYF, Chen JRT, Koh CSL et al (2020) ZIF-induced d-band modification in a bimetallic nanocatalyst: achieving over 44 % efficiency in the ambient nitrogen reduction reaction. Angew Chemie Int Ed 59:16997–17003. https://doi.org/10.1002/anie.202006071
117. Xiao L, Zhu S, Liang Y et al (2021) Effects of hydrophobic layer on selective electrochemical nitrogen fixation of self-supporting nanoporous Mo4P3 catalyst under ambient conditions. Appl Catal B Environ 286:119895. https://doi.org/10.1016/j.apcatb.2021.119895
118. Zhang J, Zhao B, Liang W et al (2020) Three-phase electrolysis by gold nanoparticle on hydrophobic interface for enhanced electrochemical nitrogen reduction reaction. Adv Sci 7:2002630. https://doi.org/10.1002/advs.202002630
119. Lai F, Zong W, He G et al (2020) N2 Electroreduction to NH3 by selenium vacancy-rich ReSe2 catalysis at an abrupt interface. Angew Chemie Int Ed 59:13320–13327. https://doi.org/10.1002/anie.202003129
120. Koh CSL, Lee HK, Fan Sim HY et al (2020) Turning water from a hindrance to the promotor of preferential electrochemical nitrogen reduction. Chem Mater 32:1674–1683. https://doi.org/10.1021/acs.chemmater.9b05313
121. Duan J, Shao D, He X et al (2021) Model MoS2@ZIF-71 interface acts as a highly active and selective electrocatalyst for catalyzing ammonia synthesis. Colloids Surfaces A Physicochem Eng Asp 619:126529. https://doi.org/10.1016/j.colsurfa.2021.126529
122. Ren Y, Yu C, Tan X et al (2021) Strategies to suppress hydrogen evolution for highly selective electrocatalytic nitrogen reduction: challenges and perspectives. Energy Environ Sci 14:1176–1193. https://doi.org/10.1039/D0EE03596C
123. Kyriakou V, Garagounis I, Vasileiou E et al (2017) Progress in the electrochemical synthesis of ammonia. Catal Today 286:2–13. https://doi.org/10.1016/j.cattod.2016.06.014
124. Garagounis I, Kyriakou V, Skodra A et al (2014) Electrochemical synthesis of ammonia in solid electrolyte cells. Front Energy Res 2
125. Xu G, Liu R, Wang J (2009) Electrochemical synthesis of ammonia using a cell with a Nafion membrane and SmFe0.7Cu0.3−xNixO3 (x = 0–0.3) cathode at atmospheric pressure and lower temperature. Sci China Ser B Chem 52:1171–1175. https://doi.org/10.1007/s11426-009-0135-7
126. Chen S, Perathoner S, Ampelli C et al (2017) Electrocatalytic synthesis of ammonia at room temperature and atmospheric pressure from water and nitrogen on a carbon-nanotube-based electrocatalyst. Angew Chemie Int Ed 56:2699–2703. https://doi.org/10.1002/anie.201609533
127. Zheng B, Xu H, Guo L et al (2020) Genomic and phenotypic diversity of carbapenemase-producing Enterobacteriaceae isolates from bacteremia in china: a multicenter epidemiological, microbiological, and genetic study. Engineering. https://doi.org/10.1016/j.eng.2020.10.015
128. Kim K, Yoo C-Y, Kim J-N et al (2016) Electrochemical synthesis of ammonia from water and nitrogen in ethylenediamine under ambient temperature and pressure. J Electrochem Soc 163:F1523–F1526. https://doi.org/10.1149/2.0741614jes
129. Kim K, Lee N, Yoo C-Y et al (2016) Communication—electrochemical reduction of nitrogen to ammonia in 2-propanol under ambient temperature and pressure. J Electrochem Soc 163:F610–F612. https://doi.org/10.1149/2.0231607jes
130. Kugler K, Luhn M, Schramm JA et al (2015) Galvanic deposition of Rh and Ru on randomly structured Ti felts for the electrochemical NH3 synthesis. Phys Chem Chem Phys 17:3768–3782. https://doi.org/10.1039/C4CP05501B
131. Durst J, Rudnev A, Dutta A et al (2015) Electrochemical CO2 reduction – a critical view on fundamentals, materials and applications. Chimia (Aarau) 69:769. https://doi.org/10.2533/chimia.2015.769
132. Zhao Y, Shi R, Bian X et al (2019) Ammonia detection methods in photocatalytic and electrocatalytic experiments: how to improve the reliability of NH3 production rates? Adv Sci 6:1802109. https://doi.org/10.1002/advs.201802109
133. LeDuy A, Samson R (1982) Testing of an ammonia ion selective electrode for ammonia nitrogen measurement in the methanogenic sludge. Biotechnol Lett 4:303–306. https://doi.org/10.1007/BF00132830
134. Thomas DH, Rey M, Jackson PE (2002) Determination of inorganic cations and ammonium in environmental waters by ion chromatography with a high-capacity cation-exchange column. J Chromatogr A 956:181–186. https://doi.org/10.1016/S0021-9673(02)00141-3
135. Yu W, Lewis NS, Gray HB, Dalleska NF (2020) Isotopically selective quantification by UPLC-MS of aqueous ammonia at submicromolar concentrations using dansyl chloride derivatization. ACS Energy Lett 5:1532–1536. https://doi.org/10.1021/acsenergylett.0c00496
136. Nielander AC, McEnaney JM, Schwalbe JA et al (2019) A versatile method for ammonia detection in a range of relevant electrolytes via direct nuclear magnetic resonance techniques. ACS Catal 9:5797–5802. https://doi.org/10.1021/acscatal.9b00358
137. Yan D, Li H, Chen C et al (2019) Defect engineering strategies for nitrogen reduction reactions under ambient conditions. Small Methods 3:1800331. https://doi.org/10.1002/smtd.201800331
138. Greenlee LF, Renner JN, Foster SL (2018) The use of controls for consistent and accurate measurements of electrocatalytic ammonia synthesis from dinitrogen. ACS Catal 8:7820–7827. https://doi.org/10.1021/acscatal.8b02120
139. Minteer SD, Christopher P, Linic S (2019) Recent developments in nitrogen reduction catalysts: a virtual issue. ACS Energy Lett 4:163–166. https://doi.org/10.1021/acsenergylett.8b02197
140. Bolleter WT, Bushman CJ, Tidwell PW (1961) Spectrophotometric determination of ammonia as indophenol. Anal Chem 33:592–594. https://doi.org/10.1021/ac60172a034
141. Giner-Sanz JJ, Leverick GM, Pérez-Herranz V, Shao-Horn Y (2020) Salicylate method for ammonia quantification in nitrogen electroreduction experiments: the correction of iron III interference.

J Electrochem Soc 167:134519. https://doi.org/10.1149/1945-7111/abbdd6
142. Hu L, Khaniya A, Wang J et al (2018) Ambient electrochemical ammonia synthesis with high selectivity on Fe/Fe oxide catalyst. ACS Catal 8:9312–9319. https://doi.org/10.1021/acscatal.8b02585
143. (2006) Determination of nitrogen species (nitrate, nitrite and ammonia ions) in environmental samples by ion chromatography. Polish J Environ Stud 15:5–18
144. Andersen SZ, Čolić V, Yang S et al (2019) A rigorous electrochemical ammonia synthesis protocol with quantitative isotope measurements. Nature 570:504–508. https://doi.org/10.1038/s41586-019-1260-x
145. Liu H, Guijarro N, Luo J (2021) The pitfalls in electrocatalytic nitrogen reduction for ammonia synthesis. J Energy Chem 61:149–154. https://doi.org/10.1016/j.jechem.2021.01.039
146. Han L, Ren Z, Ou P et al (2021) Modulating single-atom palladium sites with copper for enhanced ambient ammonia electrosynthesis. Angew Chemie Int Ed 60:345–350. https://doi.org/10.1002/anie.202010159
147. Ilyas T, Raziq F, Ilyas N et al (2022) FeNi@CNS nanocomposite as an efficient electrochemical catalyst for N2-to-NH3 conversion under ambient conditions. J Mater Sci Technol 103:59–66. https://doi.org/10.1016/j.jmst.2021.05.083
148. Chen X, Ma C, Tan Z et al (2022) One-dimensional screw-like MoS2 with oxygen partially replacing sulfur as an electrocatalyst for the N2 reduction reaction. Chem Eng J 433:134504. https://doi.org/10.1016/j.cej.2022.134504
149. Johnson D, Hunter B, Christie J et al (2022) Ti2N nitride MXene evokes the Mars-van Krevelen mechanism to achieve high selectivity for nitrogen reduction reaction. Sci Rep 12:657. https://doi.org/10.1038/s41598-021-04640-7
150. Zhao R, Wang G, Mao Y et al (2022) Li-intercalation boosted oxygen vacancies enable efficient electrochemical nitrogen reduction on ultrathin TiO2 nanosheets. Chem Eng J 430:133085. https://doi.org/10.1016/j.cej.2021.133085
151. Chang B, Li L, Shi D et al (2021) Metal-free boron carbonitride with tunable boron Lewis acid sites for enhanced nitrogen electroreduction to ammonia. Appl Catal B Environ 283:119622. https://doi.org/10.1016/j.apcatb.2020.119622
152. Zhang M, Choi C, Huo R et al (2020) Reduced graphene oxides with engineered defects enable efficient electrochemical reduction of dinitrogen to ammonia in wide pH range. Nano Energy 68:104323. https://doi.org/10.1016/j.nanoen.2019.104323
153. Li Y, Ma L, Fu Y et al (2022) Sulfurization enhancement of FeMoO4 for electrochemical ammonia synthesis with high Faradaic efficiency in neutral media. J Electroanal Chem 905:115981. https://doi.org/10.1016/j.jelechem.2021.115981
154. Li T, Xia J, Xian H et al (2022) Fe(III) grafted MoO3 nanorods for effective electrocatalytic fixation of atmospheric N2 to NH3. Int J Hydrogen Energy 47:3550–3555. https://doi.org/10.1016/j.ijhydene.2021.10.263
155. Qu Y, Dai T, Cui Y et al (2022) Tailoring electronic structure of copper nanosheets by silver doping toward highly efficient electrochemical reduction of nitrogen to ammonia. Chem Eng J 433:133752. https://doi.org/10.1016/j.cej.2021.133752
156. Tran NQ, Liu X, Cho Y et al (2022) Efficient ambient ammonia synthesis by Lewis acid pair over cobalt single atom catalyst with suppressed proton reduction. J Mater Chem A 10:8432–8439. https://doi.org/10.1039/D2TA00308B
157. Han M, Guo M, Yun Y et al (2022) Effect of heteroatom and charge reconstruction in atomically precise metal nanoclusters on electrochemical synthesis of ammonia. Adv Funct Mater 2202820. https://doi.org/10.1002/adfm.202202820
158. Zhang C, Wang Z, Lei J et al (2022) Atomic molybdenum for synthesis of ammonia with 50% Faradic efficiency. Small 18:e2106327. https://doi.org/10.1002/smll.202106327